

This is an Open Access document downloaded from ORCA, Cardiff University's institutional repository: <https://orca.cardiff.ac.uk/id/eprint/145746/>

This is the author's version of a work that was submitted to / accepted for publication.

Citation for final published version:

Niland, Andrew, Santhosh, R., Marsh, Richard and Bowen, Philip 2022. Experimental investigation of effervescent atomization: Part II. Internal flow and spray characterization with novel DARPA SUBOFF afterbody streamline aerator. *Atomization and Sprays* 32 (4) , pp. 25-51. 10.1615/AtomizSpr.2022039408

Publishers page: <https://doi.org/10.1615/AtomizSpr.2022039408>

Please note:

Changes made as a result of publishing processes such as copy-editing, formatting and page numbers may not be reflected in this version. For the definitive version of this publication, please refer to the published source. You are advised to consult the publisher's version if you wish to cite this paper.

This version is being made available in accordance with publisher policies. See <http://orca.cf.ac.uk/policies.html> for usage policies. Copyright and moral rights for publications made available in ORCA are retained by the copyright holders.



## Experimental investigation of effervescent atomization: Part II. Internal flow and spray characterization with novel DARPA SUBOFF afterbody streamline aerator

Andrew Niland<sup>a</sup>, R. Santhosh<sup>b\*</sup>, Richard Marsh<sup>a</sup>, Philip Bowen<sup>a\*</sup>

<sup>a</sup>Cardiff School of Engineering, Cardiff University, Wales CF24 3AA, UK

<sup>b</sup>Department of Mechanical Engineering, Indian Institute of Technology (BHU) Varanasi,  
Varanasi 221005, India  
[rsanthosh.mec@iitbhu.ac.in](mailto:rsanthosh.mec@iitbhu.ac.in)  
[bowenpj@cardiff.ac.uk](mailto:bowenpj@cardiff.ac.uk)

### Abstract

This experimental work reports, for the first time, observations of internal flow field involving an DARPA SUBOFF afterbody design aerator body in an *inside-out* type of effervescent atomizer. The effect of operating parameters like air-to-liquid ratio (ALR), operating pressure, aerator orifice diameter, aeration area and mixing chamber diameter on internal flow within the effervescent atomizer is studied. The effect of increasing ALR on the internal flow is quantified by identifying different gas injection mechanisms at the aerator orifice (into the mixing chamber) and two-phase mixing chamber flow regimes using high-speed shadowgraphy. In particular, it is observed that as ALR is systematically increased the gas injection mechanism transits in the following sequence: single bubbling, pulsed bubbling, elongated jetting, atomized jetting and evacuated chamber. The range of ALRs within which these mechanisms are observed are employed to draw up a flow regime map. Similar analysis on two-phase mixing chamber flow regimes yielded corresponding regime map for internal two-phase stabilized flow in the mixing chamber. The flow regime transited from bubbly flow to slug flow to churn flow and finally to annular flow as the ALR was increased. The spray characteristics (size and velocity) at the nozzle exit are reported using Phase Doppler Anemometry (PDA) measurements. It is observed that dense bubbly and bubbly-slug flow regimes produce stable sprays with droplet sizes in the range of 50-80  $\mu\text{m}$  in the range of 0.25%-1.50% ALR.

Dependence of internal flow on other parameters such as orifice aerator diameter (with constant total aerator orifice area), mixing chamber diameter and operating pressure are also studied.

Keywords: Effervescent atomization, DARPA SUBOFF afterbody streamlined aerator, gas injection regime, internal flow regimes, aerator and mixing chamber design

## Nomenclature

### Roman Characters

Symbol	Definition	Unit
$A_a$	Aeration area	$\text{m}^2$
$A_{MC}$	Mixing chamber cross-sectional area	$\text{m}^2$
$d_a$	Aerator orifice diameter	m
$d_{MC}$	Mixing chamber diameter	m
$OR_{bubbling}$	Bubbling operating range	$\text{g}^2/\text{s}^2$
$P_{op}$	Operating pressure (i.e. differential pressure between mixing chamber and atmosphere)	bar

### Acronyms

Acronym	Definition
ADARPA	DARPA SUBOFF afterbody
ALR	Air-to-liquid mass ratio

## 1. Introduction

The process of effervescent atomization represents shattering of the liquid core due to gas bubbles embedded in it due to substantial pressure drop when the two-phase fluid is forced to exit through a narrow orifice (Lefebvre et al., 1988; Lefebvre, 1988; Roesler and Lefebvre, 1989; Wang et al., 1989).

Effervescent atomisation performance is characterized by considering a number of parameters like internal flow characterization, bubble sizing, discharge coefficient, near-nozzle spray structure, spray cone angle, droplet sizing, droplet velocity etc. (Loebker and Empie, 1997; Lefebvre et al., 1988; Roesler and Lefebvre, 1989; Panchagnula and Sojka, 1999; Roesler and Lefebvre, 1989b; Chen and Lefebvre, 1994; Buckner and Sojka, 1993). Whilst some of these performance parameters generate qualitative outcomes (e.g., internal flow determination, near nozzle spray structure), the majority can be quantified by measurable and comparable evaluates (e.g., bubble size, droplet SMD and velocity). The majority of these performance parameters have been shown to vary with a number of operating parameters like liquid mass flow rate, air-to-liquid ratio (ALR) or gas-to-liquid ratio (GLR), operating pressure, aerator design, mixing chamber design, exit orifice design, liquid properties etc. The present work concerns characterization of flow inside the effervescent atomizer and study of its dependence on operating parameters like ALR, operating pressure, orifice diameter and area and mixing chamber diameter. The internal flow is known to have a significant effect on the atomisation mechanisms, where a bubbly flow is a prerequisite for effervescent atomisation (Kim and Lee, 2001; Roesler and Lefebvre, 1987; Santangelo and Sojka, 1995; Buckner and Sojka, 1991; Roesler and Lefebvre, 1988). The study of internal flow is categorized into two types. First, the study of gas injection processes at the aerator body from its orifices. Second, the visualization of stabilized gas-liquid flow in the mixing chamber. The results of internal flow visualizations are usually quantified by categorising the internal flow behaviour (both at the aerator orifice and in the mixing chamber) into flow regimes (Catlin and Swithenbank, 2001; Kim and Lee, 2001; Lörcher et al., 2005; Jobedhar, 2014; Hampel et al., 2009; Huang et al., 2008; Jedelsky and Jicha, 2013; Sun et al., 2015; Stähle et al., 2015; Gomez, 2010; Stähle et al., 2015b; Lörcher and Mewes, 2001; Liu et al., 2010; Hang et al., 2014), with some researchers extending this analysis to produce flow maps (Kim and Lee, 2001; Huang et al., 2008; Stähle et al., 2015; Lörcher and Mewes, 2001; Hang et al., 2014).

Commonly, published flow maps are referenced between studies as a technique to predict the flow regimes in effervescent atomisers where internal flow measurement may not be possible. However, in many cases, the flow maps used originate from alternative research fields and, therefore, the conditions could be unrepresentative of an effervescent atomiser (e.g., long residence time) – consequently, their reliability for predicting effervescent atomiser internal flow regime could be questioned.

There is consensus across the literature that the ALR has a significant effect on effervescent atomisation (Jedelsky et al., 2009; Petersen et al., 2001; Chin and Lefebvre, 1995; Lefebvre, 1996; Wang et al., 1989; Buckner and Sojka, 1991; Panchagnula and Sojka, 1999; Sutherland et al., 1997; Lefebvre et al., 1988), affecting both the internal flow and spray quality. Consequently, it is the most common independent parameter examined throughout the literature. The dependence of the gas injection processes at the aerator on ALR is a severely under researched area in effervescent atomisation. Jobedhar (2014) performed a basic qualitative assessment of bubble formation at the aerator for an effervescent atomiser, in which only the aerator hole spacing was varied. Sen et al. (2014) observed the effects of downstream events on bubble formation at the aerator, but their investigation was limited to a sparse bubbly flow and featured an unrepresentative atomiser design for real-world application (i.e., square cross-section mixing chamber, 1.12 m mixing length, 0.017% ALR). However, no researcher has identified the gas injection regimes at the aerator and, therefore, the relationship between the gas injection regimes at the aerator and the flow regime generated within the mixing chamber has not been established – this restricts comparability between aerator studies in alternative research fields (e.g., nuclear, waste treatment) for effervescent atomization. Despite the notable lack of research at the aerator, the effect of ALR on the internal flow regimes within the mixing chamber has been well evidenced with effervescent atomisation literature. Increasing the ALR is widely reported to transition the internal flow regime from bubbly flow, to intermittent regimes (e.g., slug flow, churn flow), and finally to annular flow (Lefebvre, 1996; Jobedhar, 2014; Huang et al., 2008; Stähle et al., 2015; Chin and Lefebvre, 1993). Generally, low ALRs are associated with small, discrete bubbles in the mixing chamber (i.e., bubbly flow) (Huang et al., 2008). The bubble size and/or number is observed to increase with ALR (Lefebvre, 1996; Jobedhar, 2014; Chin and Lefebvre, 1993) and hence the frequency of bubble coalescence increases, eventually forming large gas

slugs in the flow and instigates formation of intermittent flow regimes (e.g. slug flow, churn flow). This corresponds to experimental studies that report increased instability at 2% ALR (Santangelo and Sojka; 1995), 3% ALR (Liu et al., 2010) and 5% ALR (Sun et al., 2015; Sovani et al., 2001), which is thought to represent the critical ALRs at which transition between bubbly flow and slug flow occurs. At high ALRs, the internal flow transitions to a fully annular flow (Rahman et al., 2012; Huang et al., 2002) – this is reported to occur between 5% ALR (Santangelo and Sojka; 1995; Sun et al., 2015; Sovani et al., 2005) and 10% ALR (Mlkvik et al., 2015), with diminishing effects of ALR above 20% ALR (Sojka and Lefebvre, 1990). As a result of these differing internal flow regimes, the gas-phase expansion mechanisms have also been shown to vary from single bubbling to tree regime with increasing ALR, which results in decrease in atomiser efficiency (Sojka and Lefebvre, 1990; Jedelsky and Jicha, 2013).

This two-phase flow is then supplied to the exit orifice, where the presence of a gas-phase restricts the liquid flow area – the addition of further gas promotes this restriction and, hence, the coefficient of discharge is reported to decay with an increasing ALR (Lefebvre, 1988b; Jedelsky et al., 2009; Chin and Lefebvre, 1995; Schröder et al., 2011; Ochowiak et al., 2010; Lefebvre and Chen, 1994; Ramamurthi et al., 2009; Jedelsky et al., 2003). Hence, the use of increasing the atomising gas flow rate to achieve atomiser turndown is most effective at low ALRs.

It is unanimously agreed across the literature that the droplet SMD decreases with increasing ALR (Lefebvre, 1988b; Sojka and Lefebvre, 1990; Catlin and Swithenbank, 2001; Konstantinov, 2012; Jedelsky et al., 2009; Kim and Lee, 2001; Nielsen et al., 2006; Petersen et al., 2001; Jobehdar, 2014; Huang et al., 2008; Schröder et al., 2011; Schröder et al., 2012; Geckler et al., 2008; Broniarz-Press et al., 2010; Ochowiak et al., 2012; Ma et al., 2013; Huang et al., 2011; Ochowiak, 2012), particularly in the spray centreline (Jedelsky et al., 2009; Schröder et al., 2012). An increase in ALR acts to reduce the liquid film thickness in the exit orifice, as a greater proportion of the nozzle area is occupied by gas – as the droplet size produced is proportional to the square root of the liquid film thickness in the exit orifice (Lefebvre, 1988b), the droplet SMD decreases. An increased ALR also increases the volumetric expansion within the emerging two-phase flow and, therefore, the droplet velocity increases (Jobehdar, 2014; Huang et al., 2008; Jedelsky et al., 2008; Panchagnula and Sojka, 1999) and the spray cone

half-angle widens (Sovani et al., 2001; Jagannathan et al., 2011; Chen et al., 1994; Whitlow and Lefebvre, 1993; Wade et al., 1999).

Next, a brief review the past studies which have considered operating pressure, aerator design and mixing chamber designs in determining their effect on the effervescent atomizer performance is provided. The operating pressure is controlled by varying the injection pressure of either fluids and is a common independent variable within effervescent atomiser studies. The distribution of investigated operating pressures within the literature demonstrate that effervescent atomisers are typically operated at much lower pressures than alternative techniques – the median value of the reports surveyed is just 5 bar, which compares to an arbitrary pressure swirl atomiser for direct gasoline injection at 50 bar (Vanderwege and Hochgreb, 1998). There are, however, some effervescent atomiser studies conducted at comparably high operating pressures, for example Sovani et al. (2001) at 365 bar<sub>g</sub> and Sovani et al. (2005) at 289 bar<sub>g</sub>. The effect of increasing the operating pressure has been shown to positively affect both the internal flow and atomisation performance of an effervescent atomiser (Lefebvre, 1996; Sovani et al., 2001b; Lefebvre et al., 1988), although some researchers report this effect is minor compared to the ALR (Jedelsky et al., 2009; Petersen et al., 2001).

Increasing the operating pressure has been shown to have a favourable effect on the internal flow for effervescent atomisation. Firstly, a greater operating pressure acts to increase the liquid mass flow rate through the atomiser, which promotes bubbling at the aerator due to an increased liquid cross-flow velocity and turbulent bubble breakup in the mixing chamber (Lefebvre, 1988b). In addition, greater operating pressures compresses the gas-phase – this results in a decreased bubble size (Rahman et al., 2012), with a reduced chance of collision and hence suppressed coalescence (Yang et al., 2007). Consequently, the range of ALRs over which bubbly flow can be maintained is increased with greater operating pressures (Chin and Lefebvre, 1993). Increasing the operating pressure also promotes improved atomisation due to greater two-phase atomisation intensity (Sojka and Lefebvre, 1990) – this is generally reported to result in decreased droplet size (Lefebvre, 1988b; Sojka and Lefebvre, 1990; Konstantinov, 2012; Jedelsky et al., 2009; Petersen et al., 2001; Huang et al., 2008; Wang et al., 1989; Schröder et al., 2011; Whitlow and Lefebvre, 1993; ; Lefebvre et al., 1988; Huang et al., 2011; Wade et al., 1999; Chen et al., 1993), increased droplet velocity (Jedelsky et al.,

2008; Panchagnula and Sojka, 1999; ) and increased spray cone angle (Sovani et al., 2001; Chen et al., 1994; Whitlow and Lefebvre, 1993; Wade et al., 1999). However, some researchers report that operating pressure has an insignificant effect, particularly for high viscosity liquids (Buckner and Sojka, 1991; Geckler and Sojka, 2008) and certain ALRs thought to correspond to the annular flow regime – for example, >20% ALR (Sojka and Lefebvre, 1990), >15% ALR (Sojka et al., 1993).

Next, a discussion of past studies concerning aerator designs is provided. There are many elements of aerator design (e.g., atomiser configuration, aeration area, orifice diameter) that could affect the internal flow and subsequent atomisation performance and, therefore, there have been many reports considering elements of aerator design as an independent variable. Aerator design is considered to have a relatively minor effect on effervescent atomiser performance in comparison to other parameters (e.g. ALR and operating pressure) (Jedelsky et al., 2009; Wang et al., 1989; Lefebvre et al., 1988), however its effects have only been assessed by identifying the flow regimes formed in the mixing chamber and by analysing the spray quality – the effect of aerator design on the gas-injection processes at the aerator itself, and hence the link to the flow regimes has not been established in the effervescent atomiser literature.

The comparative merits between atomiser configurations are rarely studied, however it is reported that, due to a comparatively large liquid flow area, an *outside-in* configuration has a reduced tendency to clog (Jedelsky et al., 2009) and is therefore preferred for high flow rate applications over the *inside-out* configuration (Sovani et al., 2001b). A problem thought to exclusively affect *inside-out* configurations is the bluff body recirculation effects of the aerator body which, as previously discussed (in *Part I*), can result in the formation of a large gas void in the aerator wake (Jobedhar, 2014). It is thought, however, that bluff body recirculation can be mitigated by streamlining the aerator body to reduce the wake effect and hence improving internal flow performance – this is supported by Jobedhar (2014), who reported that gas void formation was prevented with installation of an arbitrary conical aerator tip, which resulted in increased bubbly flow homogeneity and hence improved spray stability.

It has been previously discussed that the gas velocity through the aerator orifice affects the bubbling regime at the aerator, where bubbly flow is encouraged by a low gas injection



velocity – for a given gas flow rate, this is achieved by increasing the aeration area. A wide range of aeration areas are referenced within the literature, which is thought to reflect the vast array of different fluid flow rates investigated. The result of increasing the aeration area is under-researched within effervescent atomiser literature, with its effect on gas injection and internal flow unreported, and the resulting atomisation quality disputed – some researchers reporting decreased SMD (Jedelsky et al., 2009; Chin and Lefebvre, 1995), whilst others report an insignificant effect (Broniarz-Press et al., 2010; Petersen et al., 2001). In a separate study, Jedelsky et al., (2008) reported that an increase in aeration area acts to decrease the spray cone angle.

The mixing chamber is the region in which the two-phase flow regime is stabilised, with the objective of supplying the exit orifice with the desirable flow conditions. Relatively few researchers have investigated mixing chamber design as an independent variable, predominantly thought to be due to the difficulty of varying this aspect of design without significant modifications to the experimental rig. Conventional mixing chambers have cylindrical form, with some researchers utilising rectangular designs to gain beneficial optical properties for internal flow studies (Sojka and Lefebvre, 1990; Catlin and Swithenbank, 2001; Jagannathan et al., 2011).

A wide range of mixing chamber diameters (2-30 mm) are referenced in the literature, which are shown to have weak correlation with the intended liquid flow rate – consequently, it can be concluded that there is little conformity on atomiser size between researchers. The effect of mixing chamber diameter on the internal flow has not been investigated, however it is reported to have minor influence on the subsequent two-phase atomisation (Buckner and Sojka, 1993), with Petersen et al. (2001) reporting it to have an insignificant effect on droplet SMD. Jedelsky et al., (2009), however, reported optimum performance with the mixing chamber diameter designed to be 4 times larger than the exit orifice. Consideration should be given to ensure that it is suitably small to prevent phase separation or gravitational effects to become dominant over the surface tension (i.e., conditions in which orientation does not affect atomisation) – Kim and Lee (2001) reported phase separation can be prevented by diameters less than 10mm, although the majority of effervescent atomiser studies exceed this criterion.

A number of parameters other than the ones discussed above also affect the atomizer performance. For instance, exit orifice design, liquid properties, orientation of the atomizer, atomizing gas properties etc. affect both internal flow and spray characteristics. As such, the factors reviewed above in this section do not form an exhaustive list of operating parameters affecting the internal flow field, but, are factors important from the present work point of view.

The previous paper (*Part I*) compared the internal flow of effervescent atomizer with conventional flat-end aerator body and four different streamlined aerator designs. The DARPA SUBOFF afterbody design (which is common in the conventional ship designs) was shown to be best streamline design for aerator body to produce required bubbly internal flow and minimal bluff body effect. This paper reports detailed internal flow visualization and its dependence on operating parameters i.e., ALR, operating pressure, aerator and mixing chamber design parameters, which to authors' best knowledge, has never been studied and reported before. [The work described in both \*Part I\* and \*Part II\* have been reported in Ph.D. thesis of Niland \(2017\)](#). From here on, the DARPA SUBOFF afterbody design is referred to as ADARPA in the subsequent discussion.

## **2. Experimental setup and diagnostics**

The reader is referred to *Part I* of this two-part study where the experimental facility employed is described in detail. The high-speed shadowgraphy which is employed to study internal flow and near-nozzle atomisation process has also been described there. In addition to high-speed shadowgraphy, Particle Doppler Anemometer (PDA) has been employed in the current study which is explained here.

PDA is an optical technique, using light scattering to quantify the number, size and velocity of particles within a flow. It is a time-averaged point measurement technique, which is suited for detecting small particles in the range of 0.005-1.4 mm diameter (Laakkonen et al., 2006) – hence, it is a commonly referenced spray characterisation technique within effervescent atomiser studies. A major limitation of PDA is that it is not suitable for dense spray applications, whereby the intensity of measurement light decreases due to attenuation through the spray (Gomez, 2010).

Laser light is supplied to the DualPDA system via a Coherent Innova 70 multi-line Argon Ion laser. The beam is first directed into a Dantec® 60x40 Fibre Flow transmitter, which performs the function of splitting it into six beams of three wavelengths and applying a 40 MHz frequency shift with a Bragg cell to one beam of each colour – consequently, two green (514.5 nm), two blue (488.0 nm) and two violet (476.5 nm) beams are produced. The current testing is configured in a 2D mode (i.e., detecting axial and radial velocities and droplet diameters) and, therefore, only the green and blue beams are supplied to the 112 mm Fibre PDA transmitting optics, using Dantec® 60x24 Manipulators to align the beams into the fibre optic delivery lines. The 1.5 mm diameter transmitted beams are separated by 74 mm at the optics, converging to form the measurement volume. Both transmitting and receiving optics are configured with 600 mm focal length lenses which allows sufficient clearance from the spray to prevent wetting of the equipment. The receiving optics are angled at 74° from forward scatter, which corresponds to the optimal angle for refracted scattered light for a water droplet in air (Dantec Dynamics User guide, 2006), and configured with aperture plate C, which allows for measurement of droplets up to approximately 600 µm diameter. The particle burst signals are detected by photomultipliers within the receiving optics, which are transferred and managed by a Dantec® 58N10 PDA BSA processing unit before being sent to a computer for further processing, presentation and storage by Dantec Dynamics® BSA Flow Software.

The optics are mounted onto a three-axis traverse, which allowed movement of the control volume within the spray and was automatically controlled via a connected PC with Dantec® SIZEWARE software. A suitable traverse mesh should have sufficient measurement locations to provide data representative of the spray profile, however few enough points to minimise computational and time resource. An identical traverse mesh is used across the PDA experimentation and hence the data collection is structured and consistent for all investigations. 285 individual measurement locations are examined for each individual investigation, which corresponds to 1 mm radial spacing for 25, 50, 100 and 150 mm axial displacements, and 2 mm radial spacing for 200 and 250 mm axial displacements. Axisymmetry assumption is made, resultantly, the measurements are made only in one half at a given axial section. A fixed five second sampling duration for each measurement location is adopted.

### 3. Test cases and experimental conditions

In order to characterize the internal flow of effervescent atomizer with ADARPA streamlined aerator design and to study the effect of various independent parameters on the internal flow behaviour seven different ADARPA streamlined aerators (A1A-A7A) with different aerator holes configuration as shown in Figure 1 are employed. The outer tube diameter of all aerators is 10 mm. The different aerator holes configurations are named as ' $n \times \phi m$ '. Here ' $n$ ' represents number of holes on the aerator surface of diameter ' $m$ ' which is in millimeter.

Effect of air-to-liquid (ALR) ratio on the internal flow is studied for each aerator (A1A-A7A). Various liquid flow rates employed are 30, 60, 90, 120, 180, 240 and 290 g/s. The corresponding liquid Baker parameter (the reader is referred to the *Part I* of this paper for detailed description of the Baker parameters) range is 95.5-923 kg/m<sup>2</sup>s. 5 bar gauge pressure in the atomizer is maintained by controlling the discharge valve setting (for internal flow visualisation) for each of these liquid flows or by employing interchangeable exit orifice of different diameters (for characterizing the spray). For each liquid flow rate the gas supply (from 7 bar compressed air line) is varied in increments to achieve ALR of 0.12, 0.25, 0.5, 1.0, 1.5, 2.0, 3.0, 4.0 and 5.0 %. The stabilised two-phase internal flow at each of these ALRs for every aerator is imaged using High-Speed Shadowgraphy. Each test is repeated three times to determine repeatability.

In order to study the effect of aerator orifice diameter on the internal flow the aerator configurations A1A, A2A, A3A and A6A are considered (Table 1). Each of these aerators has an outer tube diameter of 10 mm, an ADARPA streamlined body and common aeration area of 7.07 mm<sup>2</sup>. To maintain a common aeration area with differing aerator orifice diameters, the aeration orifice configuration (e.g., number of orifices, hole positioning) is required to be varied between the investigated aerators – in general, the intention of the aerator designs is to maximise the orifice spacing within a 15 mm region and 10 mm from the aerator tip.

Aeration area is investigated as independent variable by considering aerator configurations A4A (combined area of aeration holes: 1.77 mm<sup>2</sup>), A5A (area: 3.53 mm<sup>2</sup>), A6A (area: 7.07 mm<sup>2</sup>), A7A (area: 14.14 mm<sup>2</sup>) as shown in Table 1. Each of these aerators has an aerator orifice diameter of 0.75 mm, an outer tube diameter of 10 mm and a streamlined ADARPA body. The other independent parameters considered in the present study are mixing chamber diameter

and the operating pressure. These are investigated with aerator configuration A6A as depicted in the Table 1.

## **4. Results**

### ***4.1. Effect of Air-to-Liquid Ratio (ALR) on the internal flow of an 'ADARPA' atomiser***

It is observed that there is significant effect of ALR on the internal flow and near-nozzle spray characteristics of an effervescent atomiser equipped with ADARPA streamlined aerator tip. The internal flow is comprised of (a) gas injection at the aerator orifice into the mixing chamber and (b) stabilised two-phase gas-liquid flow regime in the mixing chamber. The dependence of gas injection mechanism at the aerator orifice into the mixing chamber and the resultant spray characteristics at the nozzle exit on ALR is discussed here.

#### ***4.1.1 Effect of Air-to-Liquid Ratio (ALR) on the gas injection mechanism***

Figure 2 depicts the dependence of gas injection mechanism on ALR for the aerator geometry 'A6A' (shown in Figure 1). The gas injection mechanisms for other geometries are either same or subset of the mechanisms discussed for this aerator and as such the design 'A6A' can be considered to represent a generic case. The results are comparable with all other ADARPA aerator configurations presented within this work.

The process of gas injection is observed at the aerator orifice exit (regions marked in Figure 2) and quantified for the first time for the ADARPA aerator tip-atomiser by categorising each observation into common regimes. This is performed across various fluid flow rates which resulted in the identification of five different gas injection regimes – these are a combination of the standard gas injection regimes defined previously in the literature, and a new regime defined in the current work to better describe the experimental observations. Each of these is discussed as follows:

**a. Single bubbling:** Single bubbling is observed to be the formation of individual uniformly sized bubbles, which are either sheared directly from the emerging gas-phase at the aerator orifice or detach from a short “teardrop” shaped gas neck within the peripheral liquid flow (Figure 2a) – this is in agreement with the literature descriptions (Loubière et al., 2004;

Forrester et al., 1998; Balzán et al., 2017) . Upon injection, the bubbles are drawn away from the aerator with the liquid flow into the mixing chamber.

The formation of single bubble can be explained as follows. In general, the stability of the emerging gas-phase, and hence its resistance to break-up into bubbles, is seen to decrease with: (i) High relative detachment forces: These forces are generated by strong detachment mechanisms, for example viscous forces generated by high liquid cross-flow velocity (e.g., drag, inertia), and weak restoring mechanisms, for example buoyancy. High detachment forces are encouraged by high liquid flow rates (e.g., large exit orifice diameters, increased operating pressure), small mixing chamber diameters and vertically upwards orientation. (ii) High emerging gas-liquid interface area: This increases the exposed area of the emerging gas-phase over which the detachment mechanisms act. Small aerator orifice diameters encourage high gas-liquid interface area. (iii) Low injected gas velocity: This increases the detachment rate of gas within the liquid cross-flow compared to the supply rate – this acts to suppress the generation of long gas necks connecting an otherwise detached bubble to the aerator orifice. Low injected gas velocity is a result of low gas flow rates (i.e., low ALRs) and high aeration areas. Single bubbling is observed to be promoted by the injection of a highly unstable gas-phase into a liquid continuum (i.e., highest relative detachment forces, highest emerging gas-liquid interface area and/or lowest injected gas velocity) and, hence, was promoted by low ALRs. The region of single bubbling is depicted in Figure 3 which shows different gas-phase injection regimes in the parameter space of operating liquid and gas Baker parameters. The corresponding liquid and gas flow rates are also shown.

**b. Pulse bubbling:** Pulse bubbling (Figure 2b) is observed for conditions in which the emerging gas-phase has increased stability over single bubbling i.e., increased ALR than single bubbling and, thus, gas-phase injection generates gas entities of varying size (e.g., bubble and slugs). In the majority of pulse bubbling cases, a rippling gas neck is observed to be injected into the peripheral liquid flow which resembles a series of interconnected gas entities. Given sufficient residence time and breakup mechanisms, these instabilities on the gas-liquid interface eventually gain sufficient amplitude to separate the neck into gas entities of varying size. The observations corresponding to pulse bubbling are in line with the definitions provided within the literature (Forrester et al., 1998; Balzán et al., 2017; Rigby et al., 1995). The region of pulse

bubbling is shown in the regime map (Figure 3). The combined region of single and pulse bubbling is denoted as 'bubbling' regime in Figure 3.

**c. Elongated jetting:** The elongated jetting regime is observed with increased stability of the emerging gas-phase (e.g., increased ALR), where a continuous gas jet is injected from the aerator orifice, which can chaotically break up significantly downstream of the aerator – this is in agreement with the description recently proposed by Balzán et al. (2017). Increasing the ALR through the elongated regime causes the gas jet to emerge from the aerator orifice with ever increasing momentum – this can cause it to contact with the mixing chamber, however little churning occurs. Infrequently, a small bubble may be generated due to exposure of the emerging jet to the liquid cross-flow, contact with the mixing chamber wall or shearing of the gas-liquid interface, however this is not considered to constitute as a suitable bubble formation mechanism for effervescent atomisation. Examples of elongated jetting across a variety of experiments are shown in (Figure 2c) and marked in the regime map in Figure 3.

**d. Atomised jetting:** Atomised jetting is promoted by a very stable emerging gas-phase, in which a continuous gas jet is observed to be injected into the mixing chamber. This has visibly more chaos than that associated with elongated jetting and is in agreement with the descriptions recently proposed by Balzán et al. (2017). As the ALR increases within the atomiser jetting regime, the emerging gas jet becomes ever more turbulent and the majority of cases having sufficient momentum to contact the mixing chamber wall, often with significant churning. In addition, a small number of comparatively small bubbles were frequently sheared from the gas jet upon initial exposure of the gas-phase to the liquid cross-flow, contact with the mixing chamber wall or shearing of the gas-liquid interface – this is not considered to constitute as a suitable bubble formation mechanism for effervescent atomisation. Examples of atomised jetting across a variety of experiments are shown in (Figure 2d) and marked in the regime map in Figure 3. The combined region of elongated jetting and atomised jetting is denoted as 'jetting' regime in Figure 3.

**e. Evacuated chamber:** The evacuated chamber gas injection regime is first presented in the current work to describe a condition in which phase separation is achieved immediately upon liquid injection into the atomiser, resulting in a continuous gaseous core throughout the atomiser into which the gas is directly injected at the aerator. Every observed case of

evacuated chamber occurred at a critically low liquid flow rates, whereby the liquid drag and momentum upon start-up is insufficient to displace the ambient air within the mixing chamber and hence passive bleeding of the atomiser is not achieved. Examples of evacuated chamber across a variety of experiments are shown in Figure 2e and marked in the regime map in Figure 3.

#### ***4.1.2 Effect of Air-to-Liquid Ratio (ALR) on the stabilized gas-liquid flow regime in the mixing chamber***

Figure 4 depicts the dependence of mixing chamber gas-liquid phase flow on ALR for the aerator geometry 'A6A'. The two-phase gas-liquid flow inside the mixing chamber is observed (in the regions marked in Figure 4) and quantified for the first time for the ADARPA aerator tip atomiser by categorising flow regime into six different categories – these are a combination of the standard flow regimes defined previously in the literature, and new regimes defined in the current work to better describe the experimental observations. Each of these is discussed as follows:

**a. Bubbly flow:** A bubbly flow (Figure 4a), matching the literature descriptions (Jobedhar, 2014; Furukawa and Fukano, 2001; Zhou, 2013; Usui and Sato, 1989; Bhagwat, 2011), is observed to be a homogenous two-phase flow consisting of uniformly sized bubbles within a liquid continuum, which are produced at the aerator which flow unobstructed into the mixing chamber. However, not all bubbling cases at the aerator are observed to form consistent sized bubbles – for example, pulse bubbling at relatively high ALRs is commonly observed to inject gas entities of variable size (i.e., bubbles and slugs) into the liquid cross-flow. Consequently, bubbly flow is encouraged by the injection of an unstable gas-phase which is prone to rapid break-up upon exposure to the liquid cross-flow – this is promoted by low ALRs. Therefore, bubbly flow corresponds with the majority of single bubbling cases and low ALR cases of pulse bubbling. The regime of bubbly flow is shown in Figure 5.

**b. Slug flow:** Slug flow (Figure 4b) is defined as the intermittent presence of large gas entities within a liquid continuum, which have similar diameter to the mixing chamber – this is a standard flow regime referenced within the literature (Jobedhar, 2014; Furukawa and Fukano, 2001; Zhou, 2013; Usui and Sato, 1989; Bhagwat, 2011). The formation of a slug flow



has been identified previously owing to (i) surface instabilities during co-flow gas injection (Yang et al., 2007; Cheung et al., 2012), (ii) coalescence of bubbles within the mixing chamber (Yang et al., 2007; Liao et al., 2010; Tse et al., 1998; Laakkonen et al., 2006; Shinnar and Church, 1960; Cheung et al., 2012), (iii) direct injection of gas slugs (Sen et al., 2014) and (iv) break-up of gas jets into non-uniformly sized bubbles (Forrester et al., 1998). Accordingly, in the present study, slug flow was observed (Figure 5) when gas injection is of type pulse bubbling, elongated jetting and in some cases of atomised jetting (compare Figure 3 and Figure 5). In the ALR range up to  $\sim 1.00\%$  a bubbly-slug flow is also observed (Figure 4b) wherein slug region is identified in the flow, however, towards the end of nozzle exit, the homogeneous bubbly flow prevails.

**c. Churn flow:** Churn flow (Figure 4c) is a chaotic two-phase flow in which neither phase is continuous. Every instance of churn flow within the current investigation coincided with jetting at the aerator, which mix within the mixing chamber to form a chaotic heterogeneous regime. The regime of churn flow is shown in Figure 5.

**d. Disrupted annular flow:** Disrupted annular flow (Figure 4d) is first defined in the current work to describe observations of an otherwise constant gaseous core that is regularly separated by liquid ligaments – therefore, neither fluid phases is completely continuous. It is observed under conditions of high relative buoyancy, due to the incomplete action of either coalescence or breakup. To elaborate, the formation of disrupted annular flow is encouraged by (i) incomplete coalescence: disrupted annular flow is generally observed at low liquid Baker parameter, just in excess of evacuated chamber. This corresponds to conditions at which the relative effects of buoyancy are great enough to promote coalescence of the gas-phase and thus prevent the formation of the standard intermittent flow regimes (i.e., slug flow, churn flow), however the residence is too low to enable complete coalescence into an annular flow. Consequently, residual liquid ligaments remain across the otherwise constant gas core (ii) incomplete breakup: In unusual cases, liquid ligaments are observed to be generated across a gas core due to the incomplete breakup of the gas-phase – this is observed due to gas-liquid interface surface instabilities and the interference of gas entities within the peripheral liquid flow, without separation being achieved.

**e. Annular flow:** Annular flow (Figure 4e) is widely cited within the internal flow literature (Jobedhar, 2014; Furukawa and Fukano, 2001; Zhou, 2013; Usui and Sato, 1989; Bhagwat, 2011) to be a continuous gaseous core formed in the centre of the mixing chamber surrounded by a peripheral liquid flow. Any surface instabilities generated on the gas-liquid interface or gas entitles within the liquid periphery, are not great enough to generate breakup of the gas core within the length of the mixing chamber which results in annular flow.

**f. Annular flow (liquid droplets):** Annular flow (liquid droplets) shown in Figure 4f is a unique flow regime observed in the current experimentation. It is defined by a relatively constant annular core, which encloses liquid droplets generated by dripping from the central aerator tube. The liquid droplets are occasionally seen to interfere with the liquid periphery, which can form liquid ligaments spanning the mixing chamber (akin to disrupted annular flow or churn flow). Annular flow (liquid droplets) has a tendency to occur at high liquid flow rates and ALRs, where annular flow would otherwise be expected – although there are some isolated exceptions to this rule. It is not observed for vertically upwards orientation (images not shown here for brevity) as the liquid droplets are formed under the action of gravity. This flow regime is not thought to apply to *outside-in* effervescent atomisers, as the central aerator tube from which the liquid drips would not be present.

Annular flow (liquid droplets) is not equivalent to a “wispy annular flow”, which is occasionally cited in the literature. Wispy annular flow also features liquid droplets within a gaseous core, but these are small droplets are generated due to the inner phase shearing, not large liquid droplets from dripping at the aerator. The regimes of ‘annular flow’ consisting of ‘disrupted annular flow’, ‘annular flow’ and ‘annular flow (liquid droplets)’ are shown in Figure 5.

It is observed in the present experimental study that the internal flow field is also significantly influenced by (a) aerator orifice diameter (b) aeration area (c) mixing chamber diameter and (d) operating pressure. This list presents the independent parameters considered in the present study and is by no means an exhaustive one. The effect of each of these parameters on the internal flow will be discussed in the next four sub-sections.

#### **4.1.3 Effect of Air-to-Liquid Ratio (ALR) on the spray characteristics**

While it is important to understand the effect of ALR on internal flow as described in the previous two sub-sections, it is equally important to understand its effect on spray characteristics. For this purpose, near-nozzle shadowgraphy and PDA have been employed in the present study. The spray characterisation was, however, possible only for bubbly, bubbly-slug, slug and some part of churn flow regimes i.e., for ALR range  $\sim 0$ -1.5% ALR. This is because the spray generated in flow cases at ALRs in excess of  $\sim 2.0\%$  was too unstable. However, the range of ALR amenable to PDA still depicts some interesting features that are discussed here.

Figure 6 depicts the near-nozzle spray characteristics and droplet size and velocities as ALR is varied. Particle size distribution is presented in unweighted (D10) form (i.e., Arithmetic mean diameter- AMD). This is because only  $\sim 52\%$  confidence limit was achieved for weighted average data (i.e., D32, SMD) particularly for poorly atomised sprays on the spray edge within the chosen 5s sampling duration, whereas a confidence limit of  $\sim 95\%$  is usually preferred. To achieve a  $\sim 95\%$  confidence limit in the acquisition position within the spray volume (i.e., 2D analysis – as in the present case), a very high sampling duration was determined to be necessary ( $\sim 150$ -200 s) at each of 285 measurement locations. Thus, it was considered impractical and data is presented in unweighted form. Although this is a limitation of the present study, however, it still enables identification of flow features and related spray properties. The spray edge (Figure 6) is defined as the radial position at which data rates dropped below 10% of their maximum at that axial location. The gas velocity is determined by assuming that droplet with diameter less than  $2\text{ }\mu\text{m}$  act as seeding particles within the gas flow. For locations that have no droplets satisfying this criterion, the gas velocity cannot be determined and, hence, is assumed to be zero. It is observed from Figure 6a that the internal flow at the lowest ALR (0.12% ALR) is seen to be a bubbly flow, with a low number of small bubbles existing in the liquid continuum – consequently, the single bubble atomisation is relatively irregular and hence the spray quality is poor, with a large quantity of un-atomised liquid ligaments in the spray centreline. A high number of large droplets ( $\sim 150$ - $180\text{ }\mu\text{m}$  – D10) exist in the centreline at the lowest ALR (0.12% ALR), which corresponds to the observations of a sparse bubbly flow and hence poorly atomised liquid ligaments. The associated velocities are  $\sim 35\text{ m/s}$  in the near nozzle region of  $\sim 200\text{ mm}$  from the nozzle exit. As the ALR is increased

from 0.12% to 0.25% and thereafter till ~1.00% (Figure 6b - Figure 6d) internal flow regime resulted in a bubbly and bubbly-slug flow with greater number density of small bubbles. This provided greater homogeneity – hence the regularity of the single bubble atomisation increased, which generated a more consistent and stable spray. Raising the ALR acts to increase the average gas velocity (upto ~50 m/s) within the spray, particularly in the near-nozzle region as the gas expands from the exit orifice – consequently, greater destructive mechanisms are exerted on the liquid-phase with increasing ALR and hence finer atomisation is achieved (~40-50  $\mu\text{m}$ ). Furthermore, the largest droplets (~70-80  $\mu\text{m}$ ) are seen to migrate to the spray edge as the ALR increases, as the droplet momentum due to the expanding gas carries the larger droplets away from the nozzle axis - this is in keeping with the literature reports (Jedelsky et al., 2003, Liu et al., 2011, Gomez, 2010, Jedelsky and Jícha, 2016). In addition, droplets sizes are seen to decrease with axial distance – thought to be due to the action of secondary atomisation, as droplets breakup within the ambient atmosphere. The spray characteristics at ~1.5% ALR shown in Figure 6e are evidenced when the flow regime is bubbly-slug flow (slug flow present in the flow region but the homogeneous bubbly flow prevailing towards the end of nozzle exit as shown in Figure 4b). However, consistent and stable spray with favourable single bubble atomisation is predominantly observed within 1.00% ALR. This is also the case witnessed in further sub-sections of this study where different operating parameters with different aerator configurations are employed. In most of the cases a consistent high-dense bubbly and bubbly-slug flow are witnessed within 1.00% ALR operating range.

#### **4.2. Effect of aerator orifice diameter**

The effect of aerator orifice diameter is studied by considering aerator configurations A1A, A2A, A3A and A6A. The diameter is varied between 0.75 (A6A) -3.0 (A1A) mm for a common aeration area of 7.07 mm<sup>2</sup>. The injected bubble size in the interior of effervescent atomizer is known to be proportional to the aerator orifice diameter and, therefore, a reduction in aerator orifice diameter is expected to reduce the bubble size for a given ALR and, hence, increase flow homogeneity.

Figure 7(i) shows the effect of varying the aerator orifice diameter at common 0.12% ALR and with a fully open discharge nozzle. Reducing the aerator orifice diameter (from A1A to A2A to A3A to A6A) is observed to reduce to stability of the emerging gas-phase and, therefore,

promote the detachment of bubbles. For the largest aerator orifice diameter investigated (A1A) the emerging gas-phase is relatively stable and, therefore, a gas jet is formed, which irregularly detaches from the orifice to form very large gas slug. This compares to the reduced aerator diameters (A2A, A3A and A6A- Figure 7(i)), in which the gas-phase is observed to break-up into bubbles upon exposure to the liquid cross-flow and form a bubbly flow in the mixing chamber. Due to the increasingly premature detachment of the gas-phase, the bubble size is visibly observed to reduce with decreasing aerator orifice diameter.

The purpose of an effervescent atomiser aerator is to inject the gas-phase into the liquid-phase to form uniformly sized bubbles and, hence, generate a homogenous and dense bubbly flow resulting in favourable spray characteristics. Therefore, a region in the parameter space of gas mass flow rate (ordinate) and liquid mass flow rate (abscissa) can be drawn which represent all flow setting combinations (gas and liquid mass flow rates) which produce desired dense bubbly and bubbly-slug flow regimes. These regions for the aerators discussed in this sub-section are shown in Figure 7(ii). For all of these cases, the bubbling region was restricted at: (a) high ALRs, by the transition to jetting regimes. Decreasing the aerator orifice diameter increases the ALR at which bubbling transitions to jetting, as a result of a less stable emerging gas-phase – this is thought to be caused by an increased emerging gas-liquid interface area over which the detachment mechanisms act. (b) Low liquid flow rates, by the generation of evacuated chamber. Whilst this limit was observed to marginally vary between aerator orifice diameters, the trend was not predictable – it is thought that the differences are due to the chaotic mechanisms affecting passive bleeding of the atomiser upon start-up and not the effect of aerator orifice diameter. (c) High liquid flow rates, by the flow limit of the discharge valve. Increasing the ALR acts to further restrict the valve and, hence, the liquid flow rate continually decreases. The effect of aerator orifice diameter was not seen to have a significant effect on the discharge limit.

The  $OR_{bubbling}$  (defined in *Part I* of this two-part series) for the four aerators (A1A, A2A, A3A and A6A) discussed in the present sub-section are shown in Figure 7(iii) as specific points marked with *cross marks*. It is observed that  $OR_{bubbling}$  increases with decrease in aerator orifice diameter. Further, in order to determine  $OR_{bubbling}$  at intermediate aerator diameters within the range employed in A1A -A6A, however, different from the diameters employed in A1A, A2A, A3A and A6A a curve is fit for the *cross marks* and is represented by a solid line in Figure 7(iii). This curve can be useful for designers or modelers to determine the  $OR_{bubbling}$  in

the aerator orifice diameter range considered in the present study. The spray characteristics of bubbly and bubbly-slug flows are expected to be similar to those previously described in previous sub-section and as such are not reported here.

#### **4.3. Effect of aeration area**

In this sub-section, the dependence of aeration area on the internal flow of effervescent atomizers is discussed. To consider this effect, a study of the internal flow of four different aerator configurations i.e. A4A-A7A (as previously shown in Figure 1) is accomplished. The effect of aerator aeration area on effervescent atomiser internal flow is investigated between  $1.77 \text{ mm}^2$  (A4A) -  $14.14 \text{ mm}^2$  (A7A) with an ADARPA aerator body design. In order to maintain continuity, increasing the aeration area acts to decrease the injected gas velocity. In the current investigation, the aeration area is varied for the same aerator orifice diameter by increasing the number of holes.

Figure 8(i) shows the effect of aeration area on the internal flow of an effervescent atomiser at a comparable ALR and exit orifice diameter (i.e., discharge nozzle set to fully open). At the lowest aeration area, the injected gas velocity is highest and, hence, the rate of gas supply to the emerging gas-phase is high compared to the detachment rate within the liquid cross-flow – this promotes formation of gas jets from the orifices, which intermittently detach from the orifice in a pulse bubbling regime to form a slug flow. However, the effect of increasing the aeration area decreases the injected gas velocity and, hence, is seen to reduce the length of the gas neck from which bubbles are formed – therefore, the rate of detachment increases and single bubbling and bubbly flow are promoted.

ALR range within which bubbly flow is produced for each of these aerators is shown in Figure 8(ii). The bubbling regions for all cases are limited at: (a) High ALRs, by the transition to jetting regimes. Decreasing the aeration area increased the ALR at which bubbling transitions to jetting, which indicates a less stable emerging gas-phase – this is thought to be caused by a reduced injected gas velocity, which increases the detachment rate of gas compared to the supply rate. (b) Low liquid flow rates, by the generation of evacuated chamber. Whilst this limit is observed to vary between the investigated aerator areas, the trend is not predictable – it is thought that the differences are due to the chaotic mechanisms affecting passive bleeding of the atomiser upon start-up and not the effect of aerator area. (c) High liquid flow

rates, by the flow limit of the discharge valve. Increasing the ALR acts to further restrict the valve and, hence, the liquid flow rate continually decreases. The effect of aeration area is not seen to have a significant effect on the discharge limit. Consequently, the operating range corresponding to bubbling is seen to be increased with greater aeration areas (Figure 8(ii)). The dependence of bubbling operating range ( $OR_{bubbling}$ ) in the orifice diameter range considered in the present study is shown as a non-linear curve plotted in Figure 8(iii).

#### **4.4. Effect of mixing chamber diameter**

The effect of mixing chamber diameter is studied by employing three different diameters of the mixing chamber i.e., 14 mm, 20 mm and 25 mm for a particular aerator configuration A6A as it is the generic one among the configurations considered in the present study. The effect on other aerator configurations is believed to show same characteristics as below.

Decreasing the mixing chamber diameter for given input fluid flow rates acts to increase the superficial fluid velocities and Baker parameters throughout the atomiser, including increasing the liquid cross-flow velocity around the aerator periphery. The influence of increasing the liquid cross-flow velocity encourages detachment of the forming bubbles, typically before fully expanded (Balzán et al., 2017).

Figure 9(i) shows the effect of mixing chamber diameter on the internal flow of an effervescent atomiser at a comparable ALR and exit orifice diameter (i.e., discharge nozzle set to fully open). The bubbles produced are visibly seen to decrease in size with reduction in mixing chamber diameter. For the largest mixing chambers (i.e., 20 mm and 25 mm), single bubbling is observed to form a bubbly flow within the mixing chamber. However, at the lowest mixing chamber diameter (i.e., 14 mm), the liquid cross-flow velocity is observed to be sufficient to induce bluff-body recirculation effects and, hence, bubbles are observed to coalesce in the wake region to form a small void, which sporadically detaches to generate a slug flow. Therefore, despite the reduced bluff body effect of an ADARPA aerator body design, high superficial Baker parameters are observed to generate unwanted wake effects.

Figure 9(ii) shows the bubbling regions for each case, which were limited at: (a) High ALRs, by the transition to jetting regimes. Comparing the investigated extremes (i.e., 14 mm and 25 mm), the mixing chamber diameter is seen to increase the ALR at which transition from

bubbling to jetting occurs – this is thought to be due to the increase in liquid cross-flow velocity encouraging detachment of the emerging gas-phase. However, the trend is observed to plateau at the smallest mixing chamber diameters (i.e., 14 mm and 20 mm), where transition occurs at comparable ALRs ( $\sim 1.0\%$ ). Despite this, a greater proportion of the bubbling region comprised of single bubbling cases with a reduced mixing chamber diameter, with some cases observed at 0.50% ALR for the 14 mm diameter case compared to 0.25% ALR for the 20 mm control configuration for comparable liquid flow rates – this is thought to be caused by increased detachment mechanisms promoting premature bubble detachment. (b) Low liquid flow rates, by the generation of evacuated chamber. The liquid Baker parameter for a given mass flow rate dramatically increases with a reduction in the mixing chamber diameter, the evacuated chamber regime is suppressed and bubbling promoted with a reduction in mixing chamber diameter – for example, the liquid Baker parameter at the maximum liquid mass flow rate of 289 g/s are 1890 kg/m<sup>2</sup>s for the 14 mm diameter and 589 kg/m<sup>2</sup>s for the 25 mm diameter control configuration. (c) High liquid flow rates, by the flow limit of the discharge valve. Increasing the ALR acts to further restrict the valve and hence the liquid flow rate continually decreases. The dependence of bubbling operating range on mixing chamber diameters (considered in the present study) is shown in Figure 9(iii).

#### ***4.5. Effect of operating pressure***

The effect of operating pressure on effervescent atomiser internal flow is investigated for 1, 3 and 5 bar with A6A configuration. The characteristics described below are believed to be same for other configurations as well. A greater operating pressure increases the achievable fluid flow rate through the atomiser, this relates to increased superficial fluid velocities and Baker parameters throughout the atomiser and is, therefore, expected to encourage premature detachment of the forming bubbles. In addition, an increased operating pressure acts to compress the gas-phase.

Figure 10(i) shows this effect at 0.12% ALR with the discharge nozzle setting fully open (i.e., equivalent exit orifice diameter) in which, as expected, the liquid mass flow rate is observed to increase with greater operating pressures. The bubbles produced from the aerator are visibly seen to decrease in size with increasing operating pressure which, is thought to result from a combination of factors – specifically, increased greater detachment mechanisms (i.e. increased viscous drag and inertia) and increased gas-phase compression. Consequently, in



the given cases, the effect of increasing operating pressure is seen to transition the gas injection regimes from pulse bubbling to single bubbling.

Figure 10(ii) shows the bubbling regions for both cases, which are limited at: (a) High ALRs, by the transition to jetting regimes. Whilst this limit is observed to occur at an increased ALR for the highest operating pressure, this is not reflected at lower operating pressures and hence a trend cannot be established from the current results. This is similar to the results observed when the flat-end aerator is employed. (b) Low liquid flow rates, by the generation of evacuated chamber. This limit is observed to marginally vary between the investigated operating pressures, which is thought to be caused by the chaotic mechanisms affecting passive bleeding of the atomiser upon start-up and not the effect of operating pressure. (c) High liquid flow rates, by the discharge limit of the exit nozzle. Increasing the operating pressure is seen to dramatically increase the discharge limit (i.e., increase the maximum liquid flow rates across all ALRs), where the maximum liquid mass flow rates (and equivalent liquid Baker parameters) for 1 bar<sub>g</sub>, 3 bar<sub>g</sub> and 5 bar<sub>g</sub> cases at 0% ALR are 130 g/s (413 kg/m<sup>2</sup>s), 225 g/s (717 kg/m<sup>2</sup>s) and 289 g/s (923 kg/m<sup>2</sup>s) respectively. The operating range corresponding to bubbling is seen to increase with operating pressure (considered in the present study) Figure 10(iii).

## 5. Conclusion

The present paper forms the second paper of a two-part experimental investigation of effervescent atomizers. The first part dealt with identifying the advantages of employing streamlined aerator design over conventional flat-end type of aerator. In addition, it was shown that DARPA SUBOFF afterbody design for streamlining the aerator was the best among the four different types of streamline designs investigated. This paper was the continuation of the previous part. Here, detailed characterization of the internal flow and resulting spray characteristics at the nozzle exit of the novel DARPA SUBOFF afterbody design aerator was carried out and reported for the first time.

The internal flow was imaged by employing high-speed shadowgraphy to study the effect of air-to-liquid ratio (ALR) on it. The resulting droplet size and velocity were determined using PDA. As evidenced by the past studies, the study of internal flow of atomizers form an essential part of studying their performance.

The ALR was systematically increased in the range of 0-5% to study its effect on internal flow. It was observed that the gas injection regime (at the aerator orifice) transited in mechanisms to produce bubbles, jets and finally led to evacuated chamber. The corresponding effect on the two-phase flow in the mixing chamber was observed to produce a transition from bubbly flow to slug flow to churn flow and finally to annular flow. The droplet size (Arithmetic mean diameter-  $D_{10}$ ) at the centre decreased from  $\sim 150\ \mu\text{m}$  to  $50\text{-}80\ \mu\text{m}$  when ALR was increased from 0.12% to 1.5%. The corresponding droplet velocities increased from  $\sim 35\ \text{m/s}$  to  $50\ \text{m/s}$  within the same ALR range.

Other operating parameters investigated were operating pressure (1-5 bar), aerator orifice diameter (0.75 mm – 3 mm diameter), aeration area ( $1.77\ \text{mm}^2\text{-} 14.4\ \text{mm}^2$ ) and mixing chamber diameter (14 mm, 20 mm and 25 mm). Within these conditions a parameter called ‘bubbling operating range’ ( $OR_{bubbling}$ ) was determined which quantified the range of corresponding operating condition in which the much desired bubbly flow in the effervescent atomizers is observed. Within the above mentioned range of different operating parameters the dependence of  $OR_{bubbling}$  was as follows:

- $OR_{bubbling}$  increased with decrease in aerator orifice diameter
- $OR_{bubbling}$  increased non-linearly with increase aeration areas
- $OR_{bubbling}$  decreased with increase in mixing chamber diameter
- $OR_{bubbling}$  increased with increase in operating pressure.

These relations are believed to be very useful for modellers trying simulating the internal flow of effervescent atomizers using DARPA SUBOFF afterbody design.

## References

- Balzán, M.A., Sanders, R.S. and Fleck, B.A., Bubble formation regimes during gas injection into a liquid cross flow in a conduit, *The Canadian Journal of Chemical Engineering*, vol. 95, no. 2, pp. 372-385, 2017.
- Bhagwat, S.M., Study of flow patterns and void fractions in vertical downward two phase flow, PhD, Oklahoma State University, 2011.
- Broniarz-Press, L., Ochowiak, L.M. and Woziwodzki, S., Atomization of PEO aqueous solutions in effervescent atomizers. *International Journal of Heat and Fluid Flow*, vol. 31, no. 4, pp. 651-658, 2010.
- Buckner, H.N. and Sojka, P.E., Effervescent Atomization of high-viscosity fluids: Part I. Newtonian Liquids, Atomization and Sprays, vol. 1, no. 3, pp. 239-252, 1991.
- Buckner H.E. and Sojka, P.E., Effervescent atomization of high viscosity Fluids. Part II: non-Newtonian liquids. *Atomization Sprays*, vol. 3, pp. 157-170, 1993.
- Catlin, C.A. and J. Swithenbank, Physical processes influencing effervescent atomizer performance in the slug and annular flow regimes, *Atomization and Sprays*, vol. 11, no. 5, pp. 575-595, 2001.
- Chen, S.K. and Lefebvre, A.H., Spray cone angles of effervescent atomizers. *Atomization and Sprays*, vol. 4, no. 3, pp. 275-290, 1994.
- Chen, S.K., Lefebvre, A.H. and Rollbuhler, J., Influence of ambient air pressure on effervescent atomization. *Journal of Propulsion and Power*, vol. 9, no. 1, pp. 10-15, 1993.
- Cheung, S.C.P., Yeoh, G.H., Qi, F.S., Tu, J.Y., Classification of bubbles in vertical gas-liquid flow: Part 2 - A model evaluation, *International Journal of Multiphase Flow*, vol. 39: p. 135-147, 2012.
- Chin, J.S. and Lefebvre, A.H., A design procedure for effervescent atomizers. *Journal of Engineering for Gas Turbines and Power*, vol. 117, mo. 2, pp. 266-271, 1995.
- Chin, J. and Lefebvre, A.H., Flow regimes in effervescent atomization. *Atomization and Sprays*, vol. 3, no. 3, pp. 463-475, 1993.

Dantec Dynamics, *BSA Flow Software, Installation and User's Guide*. 4.10 ed. 2006

Forrester, S.E. and Rielly, C.D., Bubble formation from cylindrical, flat and concave sections exposed to a strong liquid cross-flow. *Chemical Engineering Science*, vol. 53, no. 8, pp. 1517-1527, 1998.

Furukawa, T. and T. Fukano, Effects of liquid viscosity on flow patterns in vertical upward gas-liquid two-phase flow, *International Journal of Multiphase Flow*, vol. 27, no. 6, pp. 1109-1126, 2001.

Geckler, S.C. and Sojka, P.E., Effervescent atomization of viscoelastic liquids: Experiment and modeling. *Journal of Fluids Engineering*, Transactions of the ASME, vol. 130, no. 6, 2008.

Gomez, J., Influence of bubble size on an effervescent atomization, PhD, University of Alberta, 2010.

Hampel, U., Othál, J., Boden, S., Beyer, M., Schleicher, E., Zimmermann, W., Jicha, M., Miniature conductivity wire-mesh sensor for gas-liquid two-phase flow measurement, *Flow Measurement and Instrumentation*, vol. 20, no. 1, pp. 15-21, 2009.

Hong, M., Fleck, B.A., and Nobes, D.S., Unsteadiness of the internal flow in an effervescent atomizer nozzle. *Experiments in Fluids*, vol. 55, no. 12, pp. 1-15, 2014.

Huang, X., Wang, X.S., and Liao, G.X., Visualization of two phase flow inside an effervescent atomizer, *Journal of Visualization*, vol. 11, no. 4, pp. 299-308, 2008.

Huang, X., Wang, X.S. and Liao, G.X., Characterization of an effervescent atomization water mist nozzle and its fire suppression tests, *Proceedings of the Combustion Institute*, vol. 33, no. 2, pp. 2573-2579, 2011.

Jagannathan, T.K., R. Nagarajan, and K. Ramamurthi, Effect of ultrasound on bubble breakup within the mixing chamber of an effervescent atomizer, *Chemical Engineering and Processing: Process Intensification*, vol. 50, no. 3, pp. 305-315, 2011

Jedelsky, J., M. Jicha, and J. Slama, Characterization of spray generated by multihole effervescent atomizer and comparison with standard Y-jet atomizer, *Proc. of the Ninth*

*International Conference on Liquid Atomization and Spray Systems (ICLASS-2003)*, Sorrento, Italy, 2003.

Jedelsky, J., Landsmann, M., Jicha, M., Kuritka, I., Effervescent Atomizer: Influence of the Operation Conditions and Internal Geometry on Spray Structure; Study Using PIV-PLIF, Proc. ILASS, Como Lake, Italy, 2008.

Jedelsky, J., Miroslav, J., Slama, J. and Otahal, J., Development of an effervescent atomizer for industrial burners, *Energy and Fuels*, vol. 23, no. 12, pp. 6121-6130, 2009.

Jedelsky, J. and Jicha, M., Energy conversion during effervescent atomization, *Fuel*, vol. 111, pp. 836-844, 2013.

Jedelský, J. and Jícha, M., Spray characteristics and liquid distribution of multi-hole effervescent atomisers for industrial burners, *Applied Thermal Engineering*, vol. 96, pp. 286-296, 2016.

Jobehdar, M.H., Experimental Study of Two-Phase Flow in a Liquid Cross-Flow and an Effervescent Atomizer, PhD, University of Western Ontario, 2014.

Kim, J.Y. and S.Y. Lee, Dependence of spraying performance on the internal flow pattern in effervescent atomizers, *Atomization and Sprays*, vol. 11, no. 6, pp. 735-756, 2001.

Konstantinov, D.D., Effervescent Atomisation for Complex Fuels including Bio-Fuels, PhD, University of Wales Cardiff, 2012.

Laakkonen, M., V. Alopaeus, and J. Aittamaa, Validation of bubble breakage, coalescence and mass transfer models for gas-liquid dispersion in agitated vessel, *Chemical Engineering Science*, vol. 61, no. 1, pp. 218-228, 2006.

Lörcher, M., F. Schmidt, and D. Mewes, Effervescent atomization of liquids, *Atomization and Sprays*, vol. 15, no. 2, pp. 145-168, 2005.

Lefebvre AH., A novel method of atomization with potential gas turbine application, *Defence Science Journal*, vol. 38, pp. 353-361, 1988.

Lefebvre, A.H., Wang, X.F., and Martin, C.A., Spray characteristics of aerated-liquid pressure atomizers. *Journal of Propulsion and Power*, vol. 4, no. 4, pp. 293-298, 1988.

- Lefebvre, A.H. and Chen, S.K., Discharge Coefficients for Plain-Orifice Effervescent Atomizers, *Atomization and Sprays*, vol. 4, no. 3, pp. 275-290, 1994.
- Lefebvre, A.H., Some recent developments in twin-fluid atomization. *Particle and Particle Systems Characterization*, vol. 13, no. 3, pp. 205-216, 1996
- Liao, Y. and Lucas, D., A literature review on mechanisms and models for the coalescence process of fluid particles. *Chemical Engineering Science*, vol. 65, no. 10, pp. 2851-2864, 2010.
- Liu, M., Duan, Y., and Zhang, T., Evaluation of effervescent atomizer internal design on the spray unsteadiness using a phase/Doppler particle analyzer. *Experimental Thermal and Fluid Science*, vol. 34, no. (6), pp. 657-665, 2010.
- Liu, M., Duan, Y., Zhang, T. and Xu, Y., Evaluation of unsteadiness in effervescent sprays by analysis of droplet arrival statistics - The influence of fluids properties and atomizer internal design, *Experimental Thermal and Fluid Science*, vol. 35, no. 1, pp. 190-198, 2011.
- Loebker D, Empie H.J, High mass Flow-rate effervescent spraying of high viscosity Newtonian liquid, *Proceedings of the 10th Annual Conference on Liquid Atomization and Spray Systems*, Ottawa, ON, pp. 253-257, 1997
- Lörcher, M. and Mewes, D., Atomization of liquids by two-phase gas-liquid flow through a plain-orifice nozzle: Flow regimes inside the nozzle. *Chemical Engineering & Technology*, vol. 24, no. 2, pp. 167-172, 2001.
- Loubière, K., Castagnede, V., Hebrard, G. and Roustan, M., Bubble formation at a flexible orifice with liquid cross-flow. *Chemical Engineering and Processing: Process Intensification*, vol. 43, no. 6, pp. 717-725, 2004.
- Ma, X., Duan, Y and Liu, M., Atomization of petroleum-coke sludge slurry using effervescent atomizer. *Experimental Thermal and Fluid Science*, vol. 46, pp. 131-138, 2013.
- Mlkvik, M., Stahle, P., Schuchmann, H.P., Gaukel, V., Jedelsky, J., Jicha, M., Twin-fluid atomization of viscous liquids: The effect of atomizer construction on breakup process,

- spray stability and droplet size. *International Journal of Multiphase Flow*, vol. 77, pp. 19-31, 2015.
- Mostafa, A., Fouad, M., Enayet, M., Osman, S., Measurements of spray characteristics produced by effervescent atomizers, *40th AIAA/ASME/SAE/ASEE Joint Propulsion Conference and Exhibit*, Fort Lauderdale, FL, 2004 (<https://doi.org/10.2514/6.2004-3378>)
- Nielsen, A. F., Poul, B., Kristensen, H.G., Kristensen, J., Hovgaard, L., Investigation and comparison of performance of effervescent and standard pneumatic atomizer intended for soluble aqueous coating. *Pharmaceutical Development and Technology*, vol. 11, no. 2, pp. 243-253, 2006.
- Niland, A., Internal flow studies for the characterisation and optimisation of an effervescent atomiser, PhD Thesis, Cardiff University, 2017.
- Ochowiak, M., Broniarz-Press, L and Rozanski, J., The discharge coefficient of effervescent atomizers. *Experimental Thermal and Fluid Science*, vol. 34, no. 8, pp. 1316-1323, 2010.
- Ochowiak, M., The effervescent atomization of oil-in-water emulsions. *Chemical Engineering and Processing: Process Intensification*, vol. 52, pp. 92-101, 2012.
- Ochowiak, M., Broniarz-Press, L., Rozanska, S., Rozanski, J., The effect of extensional viscosity on the effervescent atomization of polyacrylamide solutions. *Journal of Industrial and Engineering Chemistry*, vol. 18, no. 6, pp. 2028-2035, 2012.
- Panchagnula, M.V. and Sojka, P.E., Spatial droplet velocity and size profiles in effervescent atomizer-produced sprays. *Fuel*, vol. 78, no. 6, pp. 729-741, 1999
- Petersen, F.J, Worts, O., Schaefer, T., Sojka, P.E., Design and Atomization Properties for an Inside-Out Type Effervescent Atomizer, *Drug Development and Industrial Pharmacy*, vol. 30, no. 3, pp. 319-326, 2004.
- Petersen, F.J., Worts, O., Sojka, P. E., Effervescent atomization of aqueous polymer solutions and dispersions, *Pharmaceutical Development and Technology*, vol. 6, no. 2, pp. 201-210, 2001.

- Rahman, M.A., Balzan, M., Heidrick, T., Fleck, B.A., Effects of the gas phase molecular weight and bubble size on effervescent atomization, *International Journal of Multiphase Flow*, vol. 38, no. 1, pp. 35-52, 2012.
- Ramamurthi, K., Sarkar, U.K., and Raghunandan, B.N., Performance characteristics of effervescent atomizer in different flow regimes. *Atomization and Sprays*, vol. 19, no. 1, pp. 41-56, 2009.
- Rigby, G.D., Evans, G.M and Jameson, G.J., Modelling of gas flow from a submerged orifice in liquid cross-flow, *Chemical Engineering Research and Design*, vol. 73, no. A3, pp. 234-240, 1995.
- Roesler T.C, Lefebvre A.H., Studies on aerated-liquid atomization, *Int J Turbo Jet Engines* vol. 6, pp. 221-230, 1989.
- Roesler T.C, Lefebvre A.H., Photographic studies on aerated liquid atomization, combustion fundamentals and applications, *Proceedings of the Meeting of the Central States Section of the Combustion Institute*, Indianapolis, Indiana, Paper 3, 1988.
- Santangelo, P.J. and P.E. Sojka, A Holographic Investigation of the near-nozzle structure of an Effervescent atomizer-produced spray, *Atomization and Sprays*, vol. 5 no. 2, pp. 137-155, 1995.
- Schröder, J., Kraus, S., Rocha, B.B., Gaukal, V., Schuchmann, H.P., Characterization of gelatinized corn starch suspensions and resulting drop size distributions after effervescent atomization, *Journal of Food Engineering*, vol. 105, no. 4, pp. 656-662, 2011.
- Schröder, J., Kleinhans, A., Serfert, Y., Drusch, S., Karbstein, H. P., Gaukel, V., Viscosity ratio: A key factor for control of oil drop size distribution in effervescent atomization of oil-in-water emulsions. *Journal of Food Engineering*, vol. 111, no. 2, pp. 265-271, 2012.
- Sen, D., Balzan, M.A., Nobes, D.S., Fleck, B.A., Bubble formation and flow instability in an effervescent atomizer. *Journal of Visualization*, vol. 17, no. 2, pp. 113-122, 2014.



- Shinnar, R. and J.M. Church, Statistical Theories of Turbulence in Predicting Particle Size in Agitated Dispersions, *Industrial & Engineering Chemistry*, vol. 52, no. 3, pp. 253-256, 1960.
- Sojka, P.E. and Lefebvre, A.H., A Novel Method of Atomizing Coal-Water Slurry Fuels, US DOE, Pittsburgh, Tech. Rep. DOE/PC/79913-T4, May 1990.
- Sojka, P.E. and H.N. Buckner, Effervescent Atomization of high-viscosity fluids: Part II. Non-Newtonian Liquids, *Atomization and Sprays*, vol. 3, no. 2, pp. 157-170, 1993.
- Sovani, S.D., P.E. Sojka, and A.H. Lefebvre, Effervescent atomization, *Progress in Energy and Combustion Science*, vol. 27, no. 4, pp. 483-521, 2001.
- Sovani, S.D., Chou, E., Sojka, P.E., Gore, J.P., Eckerle, W.A., Crofts, J.D., High pressure effervescent atomization: Effect of ambient pressure on spray cone angle, *Fuel*, vol. 80, no. 3, pp. 427-435, 2001.
- Sovani, S.D., Crofts, J.D., Sojka, P.E., Gore, J.P., Eckerle, W.A., Structure and steady-state spray performance of an effervescent diesel injector. *Fuel*, vol. 84, no. 12-13, pp. 1503-1514, 2005.
- Stähle, P., Gaukel, V., and Schuchmann, H.P., Investigation on the Applicability of the Effervescent Atomizer in Spray Drying of Foods: Influence of Liquid Viscosity on Nozzle Internal Two-Phase Flow and Spray Characteristics, *Journal of Food Process Engineering*, vol. 38, no. 5, pp. 474-487, 2015.
- Stähle, P., Gaukel, V., and Schuchmann, H.P., Comparison of an Effervescent Nozzle and a Proposed Air-Core-Liquid-Ring (ACLR) Nozzle for Atomization of Viscous Food Liquids at Low Air Consumption. *Journal of Food Process Engineering*, vol. 40, no. 1. E12268, 2015.
- Sun, C., Ning, Z., Lv, M., Yan, K., Fu, J., Time-frequency analysis of acoustic and unsteadiness evaluation in effervescent sprays, *Chemical Engineering Science*, vol. 127, pp. 115-125, 2015.

- Sutherland, J.J., Sojka, P.E. and Plesniak, M.W., Ligament-controlled effervescent atomization. *Atomization and Sprays*, vol. 7, no. 4, pp. 383-406, 1997.
- Tse, K., Martin, T., Mcfarlane, C.M., Nienow, A.W., Visualisation of bubble coalescence in a coalescence cell, a stirred tank and a bubble column, *Chemical Engineering Science*, vol. 53, no. 23, pp. 4031-4036, 1998.
- Usui, K. and K. Sato, Vertically downward two-phase flow, (I) Void distribution and average void fraction, *Journal of Nuclear Science and Technology*, vol. 26, no. 7, pp. 670-680, 1989.
- Vanderwege, B.A. and Hochgreb, S., *The effect of fuel volatility on sprays from high-pressure swirl injectors*. Symposium (International) on Combustion, vol. 27, no. 2, pp. 1865-1871, 1998.
- Wade, R.A., Weerts, J.M., Gore, J.P., Eckerle, W.A., Effervescent atomization at injection pressures in the MPa range. *Atomization and Sprays*, vol. 9, no. 6, pp. 651-66, 1999.
- Whitlow, J.D. and Lefebvre, A.H., Effervescent Atomizer Operation and Spray Characteristics, *Atomization and Sprays*, vol. 3, no. 6, pp. 137-155, 1993.
- Yang, G.Q., B. Du, and L.S. Fan, Bubble formation and dynamics in gas-liquid-solid fluidization- A review, *Chemical Engineering Science*, vol. 62, no.1-2: pp. 2-27, 2007.
- Zhou, J., Flow patterns in vertical air/water flow with and without surfactant, PhD, University of Dayton, 2013.

## Figures and Table

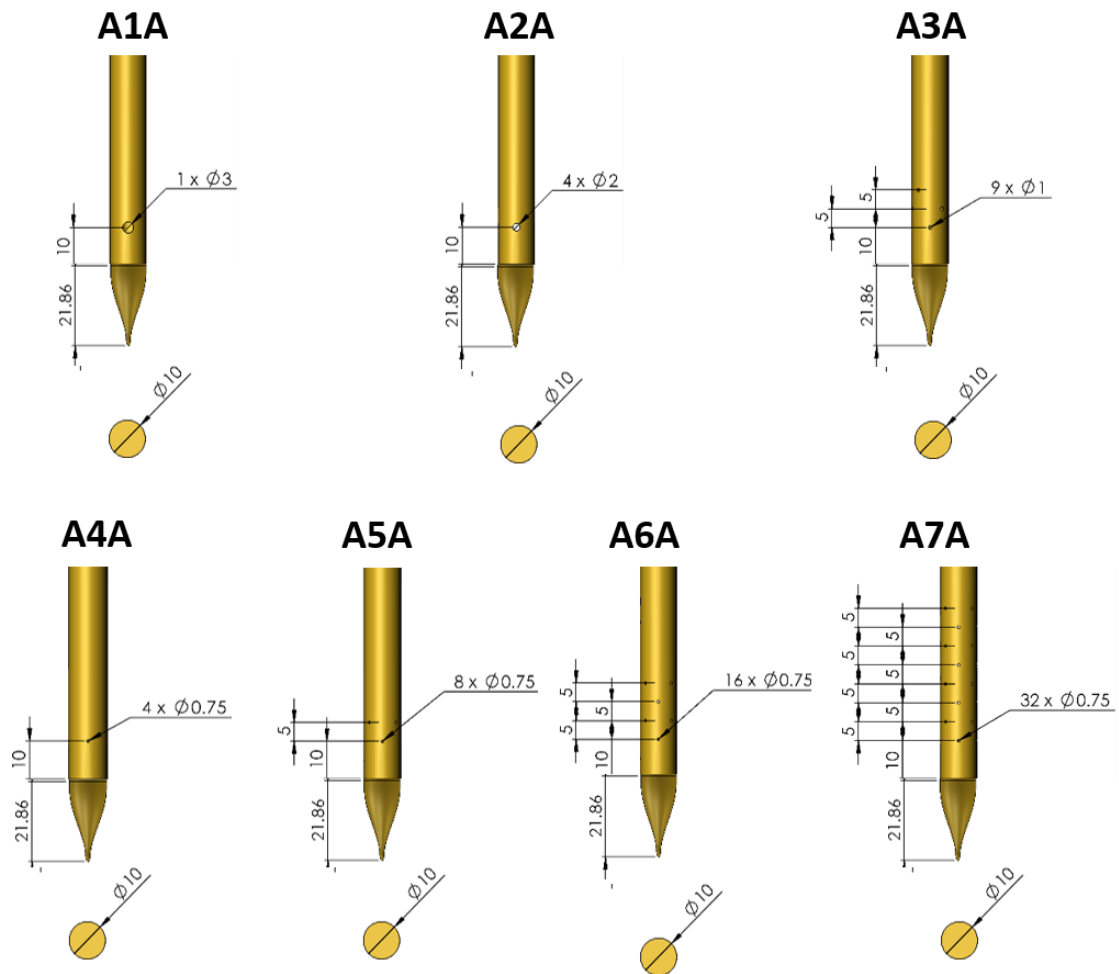


Figure 1. Different ADARPA aerator body configurations employed in the present study

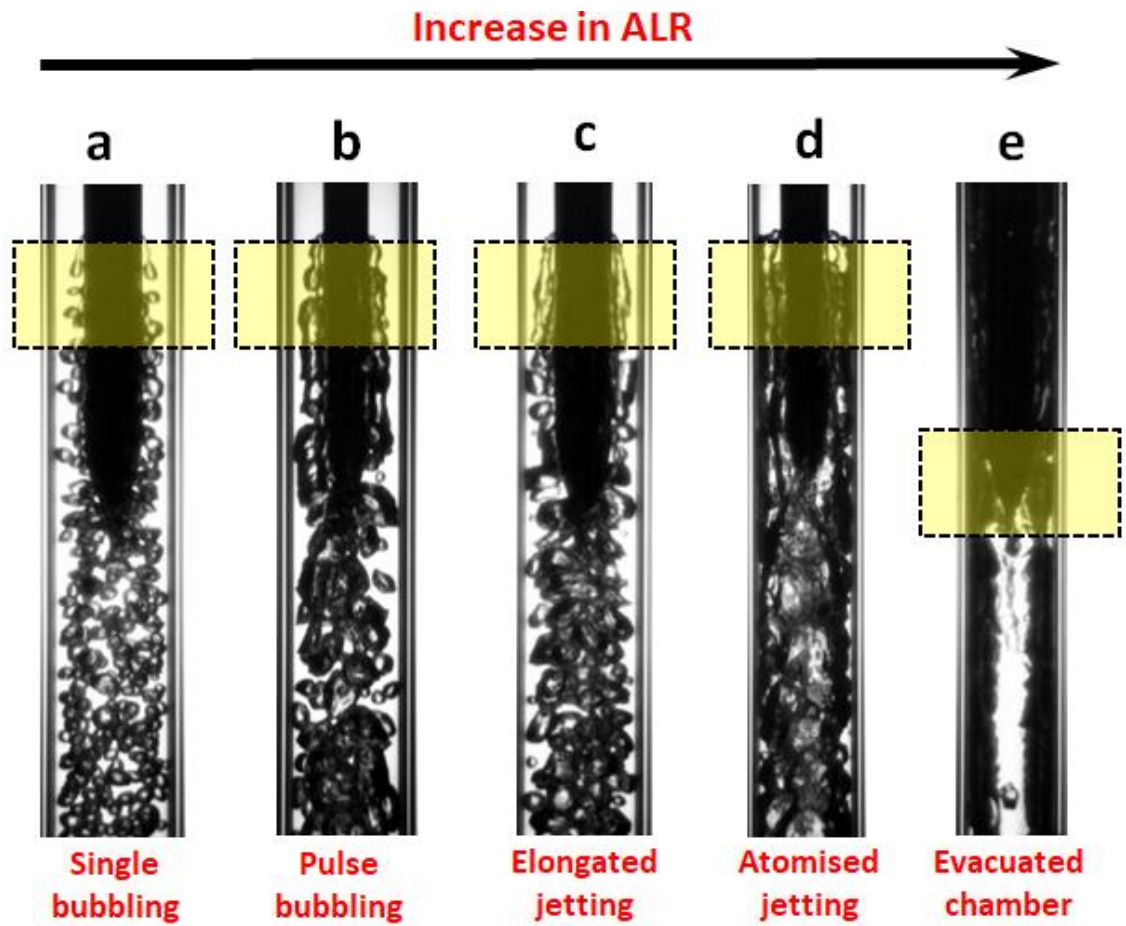


Figure 2. Representative images depicting the effect of ALR on gas injection mechanism for the aerator geometry A6A: a) 0.185% ALR; b) 0.48% ALR; c) 1.5% ALR; d) 2.04% ALR; e) 4.5% ALR.

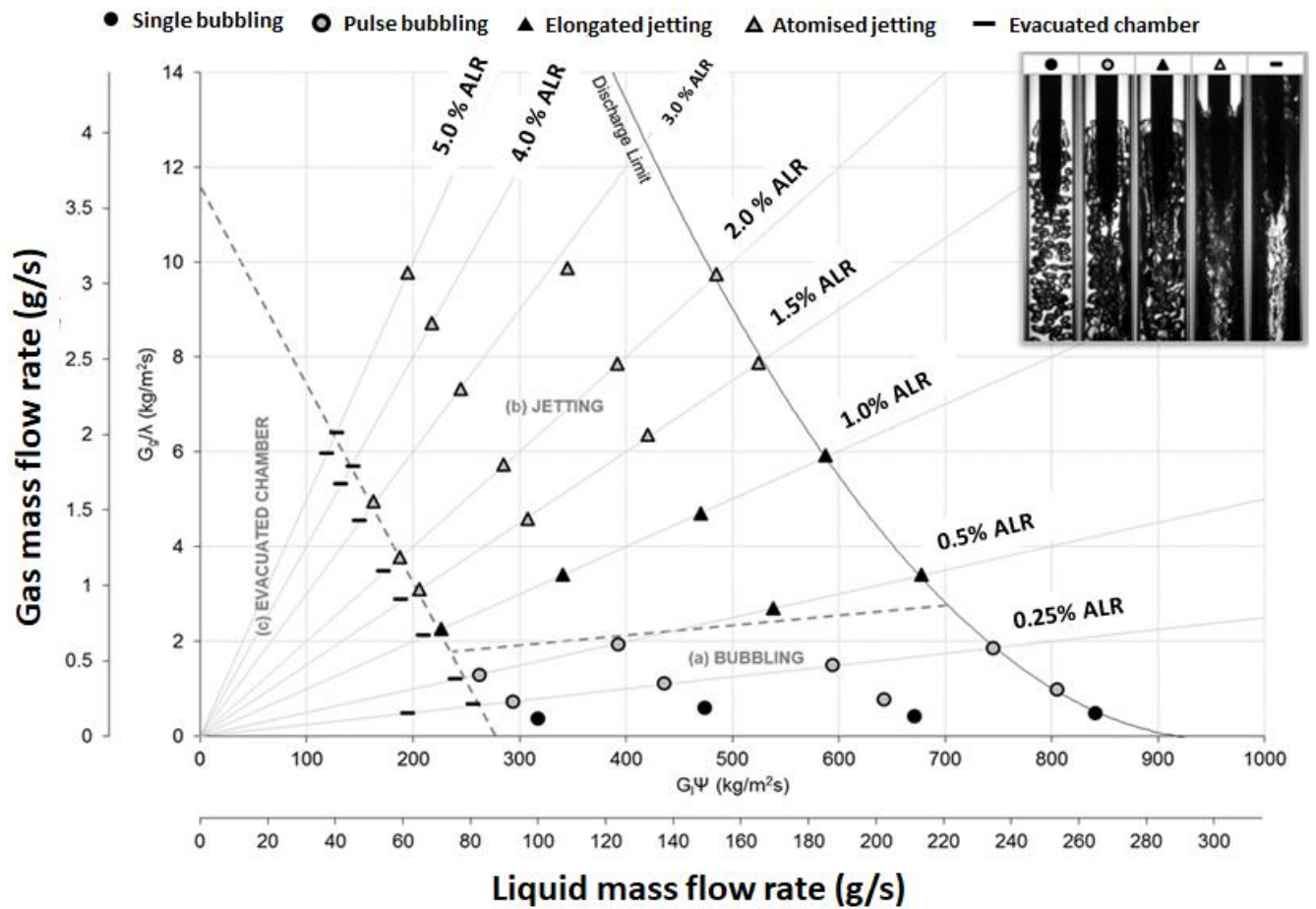


Figure 3. Gas injection regime map for the aerator configuration A6A

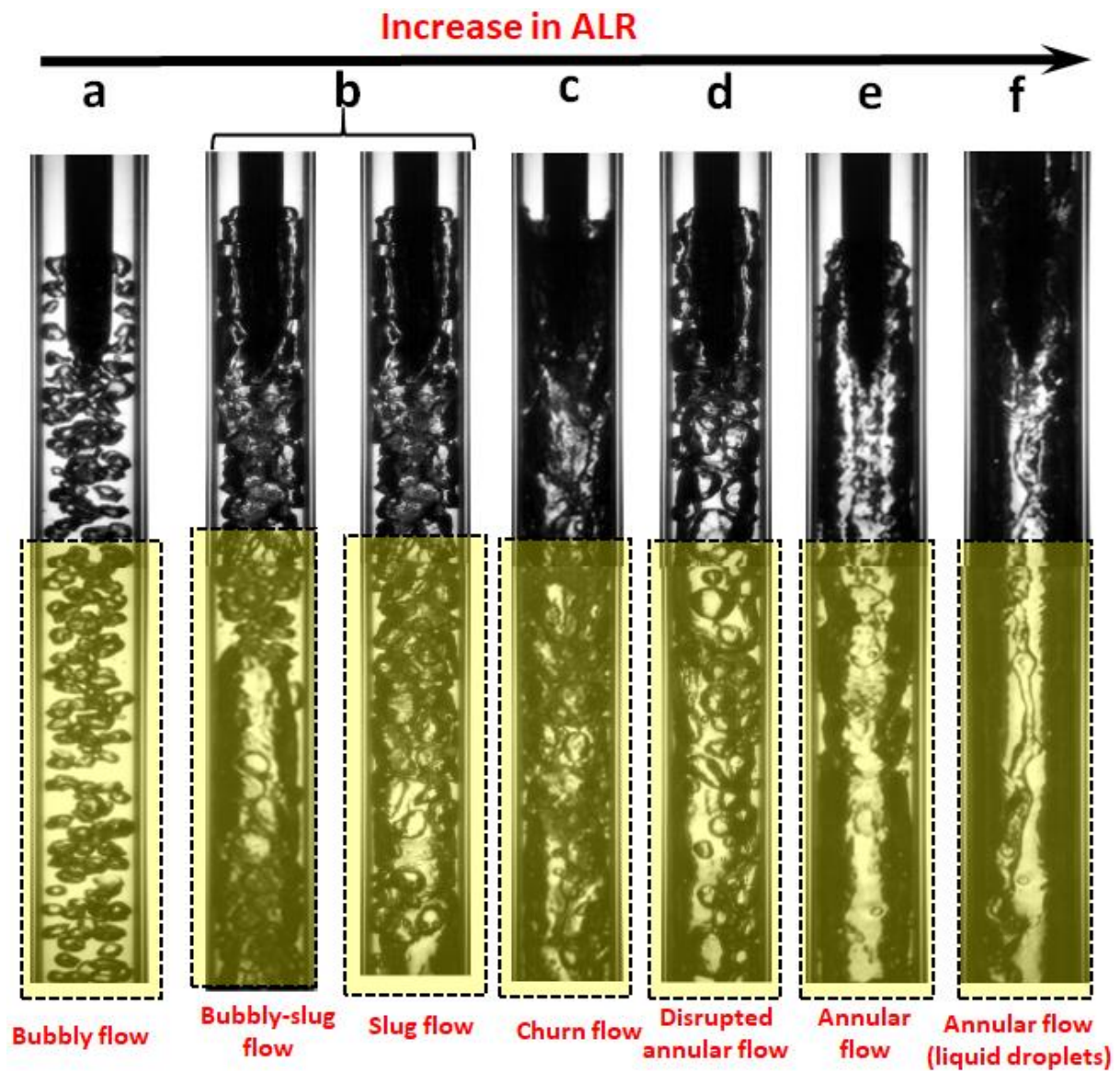


Figure 4. Representative images depicting the effect of ALR on two-phase mixing chamber flow regime for the aerator geometry A6A: a) 0.135% ALR; b) 0.5% ALR; c) 1.75% ALR; d) 1.85% ALR; e) 1.9% ALR; f) 4.5% ALR.

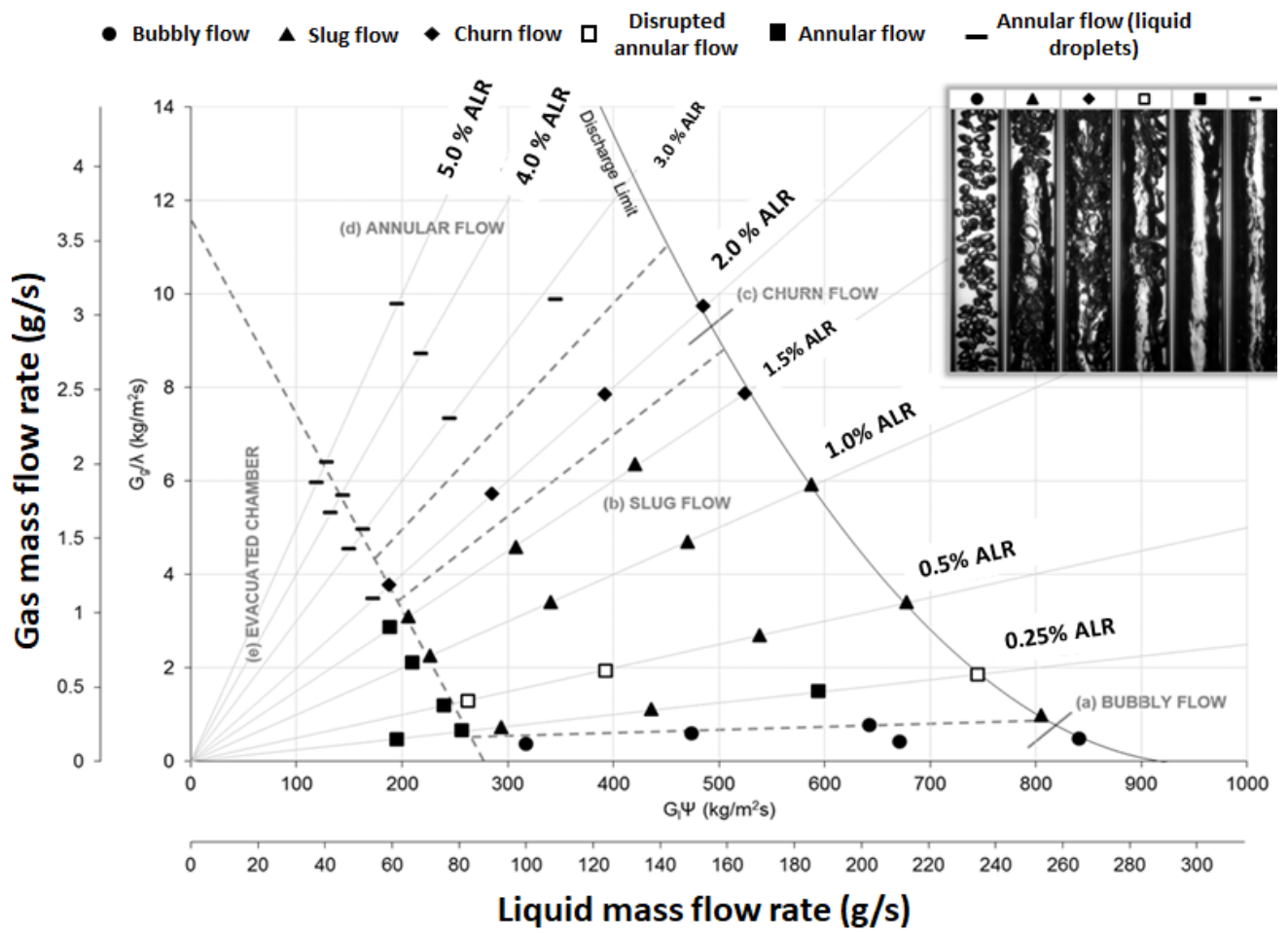


Figure 5. Mixing chamber flow regime map for the aerator configuration A6A



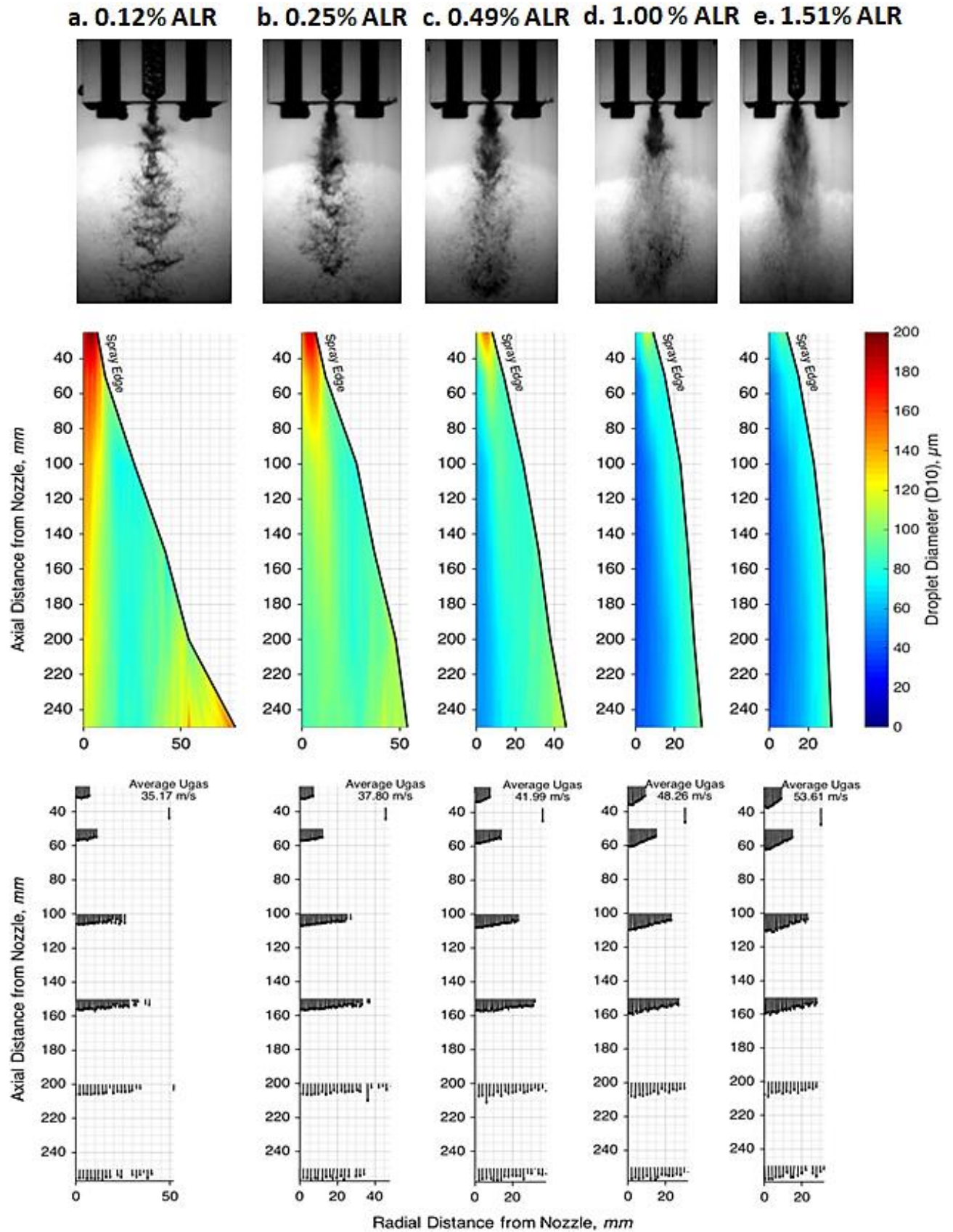


Figure 6. Near nozzle atomisation (top row), droplet spray size profiles (middle row) and gas velocity quiver plot (bottom row) for a) 0.12% ALR; b) 0.25% ALR; c) 0.49% ALR; d) 1.00% ALR; e) 1.51% ALR



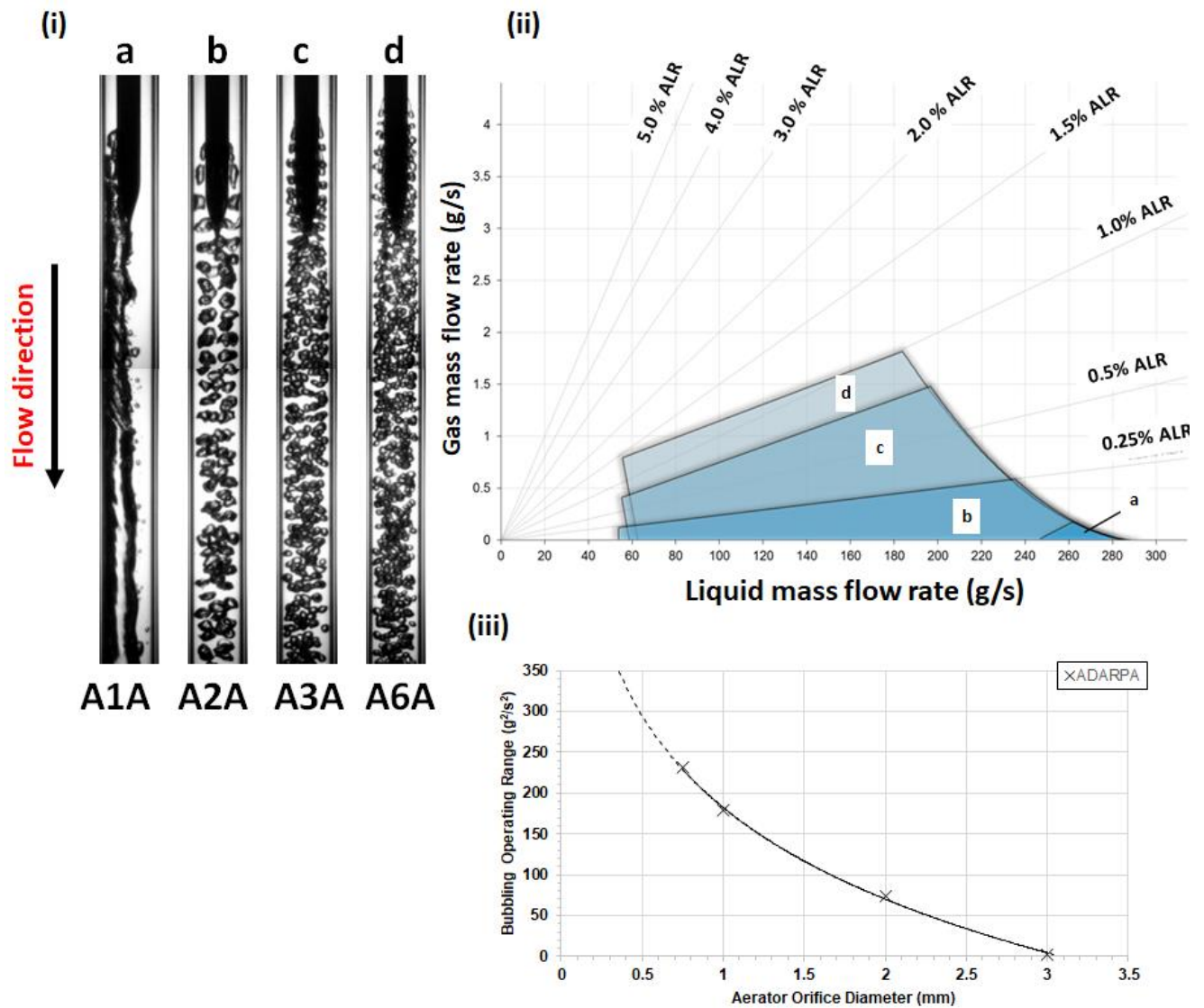


Figure 7. (i) Comparable observations with varying aerator orifice diameter: a) Aerator A1A – 1 x 3.0 mm, flow rate: 252 g/s, 0.12% ALR; b) Aerator A2A – 4 x 2.0 mm, 252 g/s, 0.12% ALR; c) Aerator A3A – 9 x 1.0 mm, 252 g/s, 0.12% ALR; d) Aerator A6A – 16 x 0.75 mm, 251 g/s, 0.12% ALR. Liquid Baker parameter for all four cases is around: 802.54  $\text{kg}/\text{m}^2\text{s}$  (ii) Effect of aerator orifice diameter on bubbling operating range: a) aerator A1A; b) aerator A2A; c) aerator A3A; d) aerator A6A. (iii) Dependence of aerator orifice diameter on bubbling operating range.

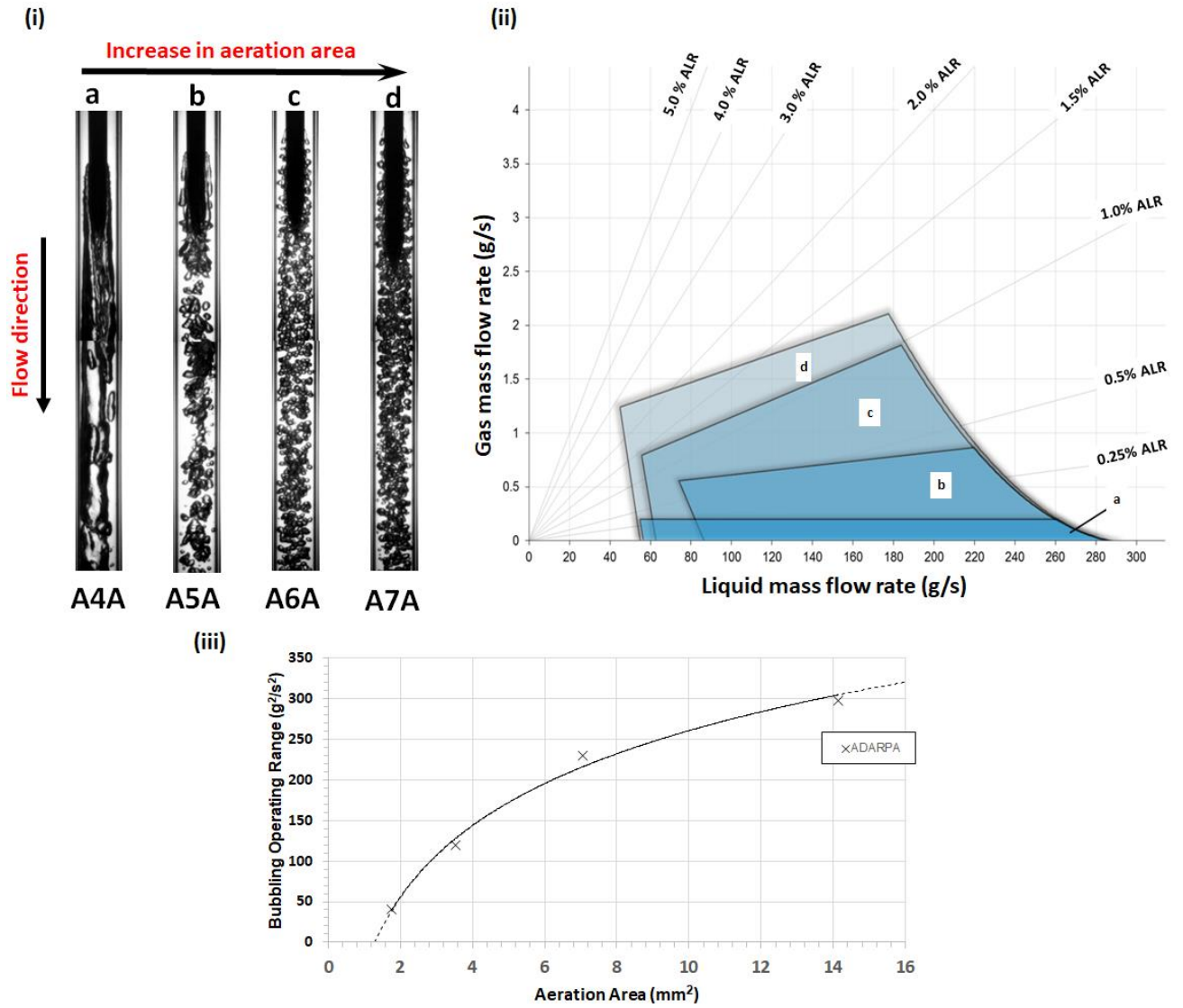


Figure 8. (i) Comparable observations of varying aeration area: a) Aerator A4A –  $1.77 \text{ mm}^2$ ,  $253 \text{ g/s}$ ,  $0.12\% \text{ ALR}$ ; b) Aerator A5A –  $3.53 \text{ mm}^2$ ,  $253 \text{ g/s}$ ,  $0.12\% \text{ ALR}$ ; c) Aerator A6A –  $7.07 \text{ mm}^2$ ,  $251 \text{ g/s}$ ,  $0.12\% \text{ ALR}$ ; d) Aerator A7A –  $14.14 \text{ mm}^2$ ,  $252 \text{ g/s}$ ,  $0.12\% \text{ ALR}$ . Liquid Baker parameter for all four cases is around:  $802.54 \text{ kg/m}^2\text{s}$ . (ii) Effect of aerator area on bubbling operating range: a) aerator A4A; b) aerator A5A; c) aerator A6A; d) aerator A7A. (iii) Dependence of aerator area on bubbling operating range.

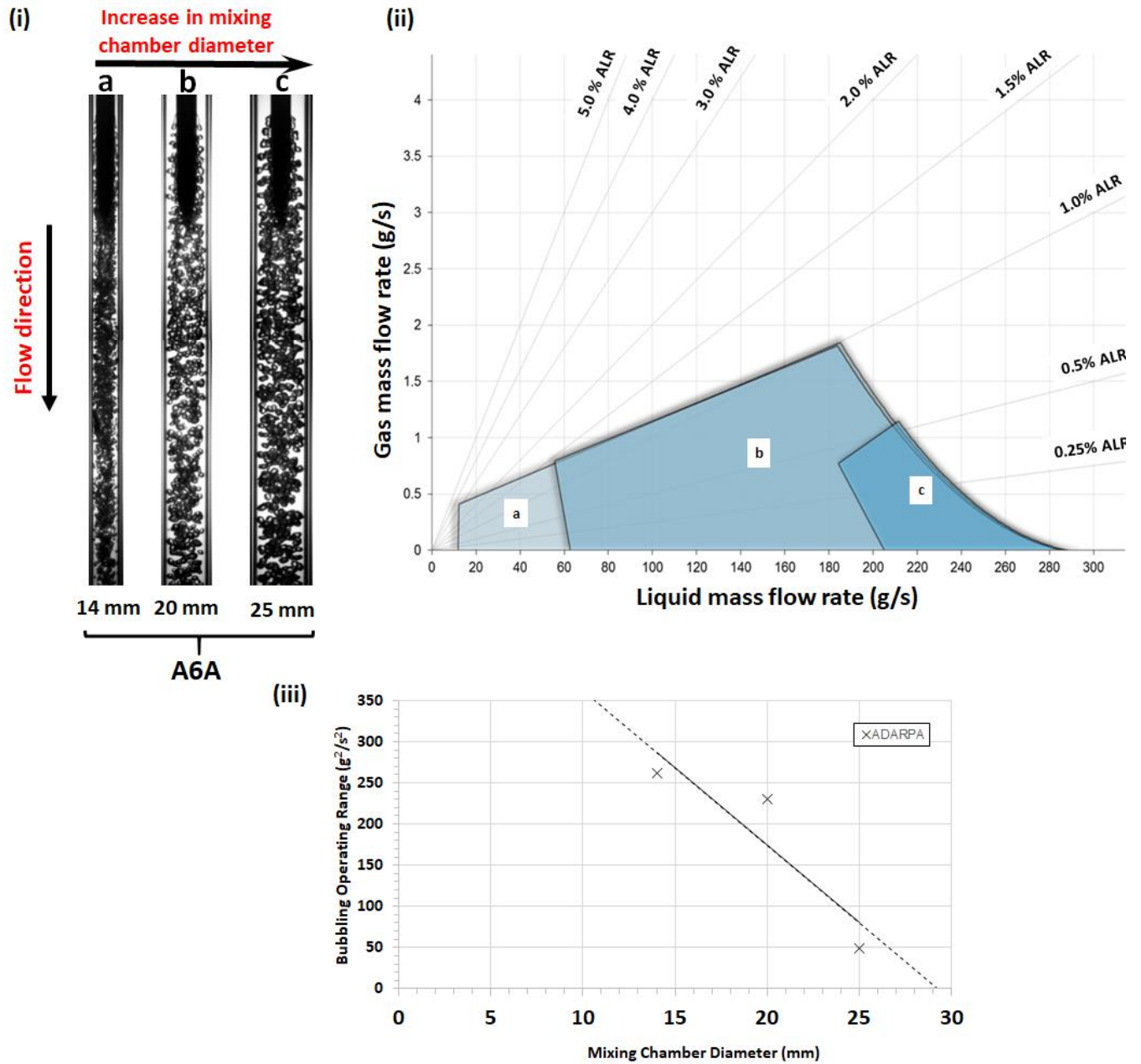


Figure 9. (i) Comparable observations of varying mixing chamber diameter for A6A: a) 14 mm diameter, 253 g/s, 0.12% ALR; b) 20 mm diameter, 251 g/s, 0.12% ALR; c) 25 mm diameter, 251 g/s, 0.12% ALR. Liquid Baker parameter for all four cases is around:  $802.54 \text{ kg/m}^2\text{s}$ . (ii) Effect of mixing chamber diameter on bubbling operating range, with respect to the fluid mass flow rates: a) 14 mm diameter (b) 20 mm diameter; c) 25 mm diameter. (iii) Dependence of mixing chamber diameter on bubbling operating range.

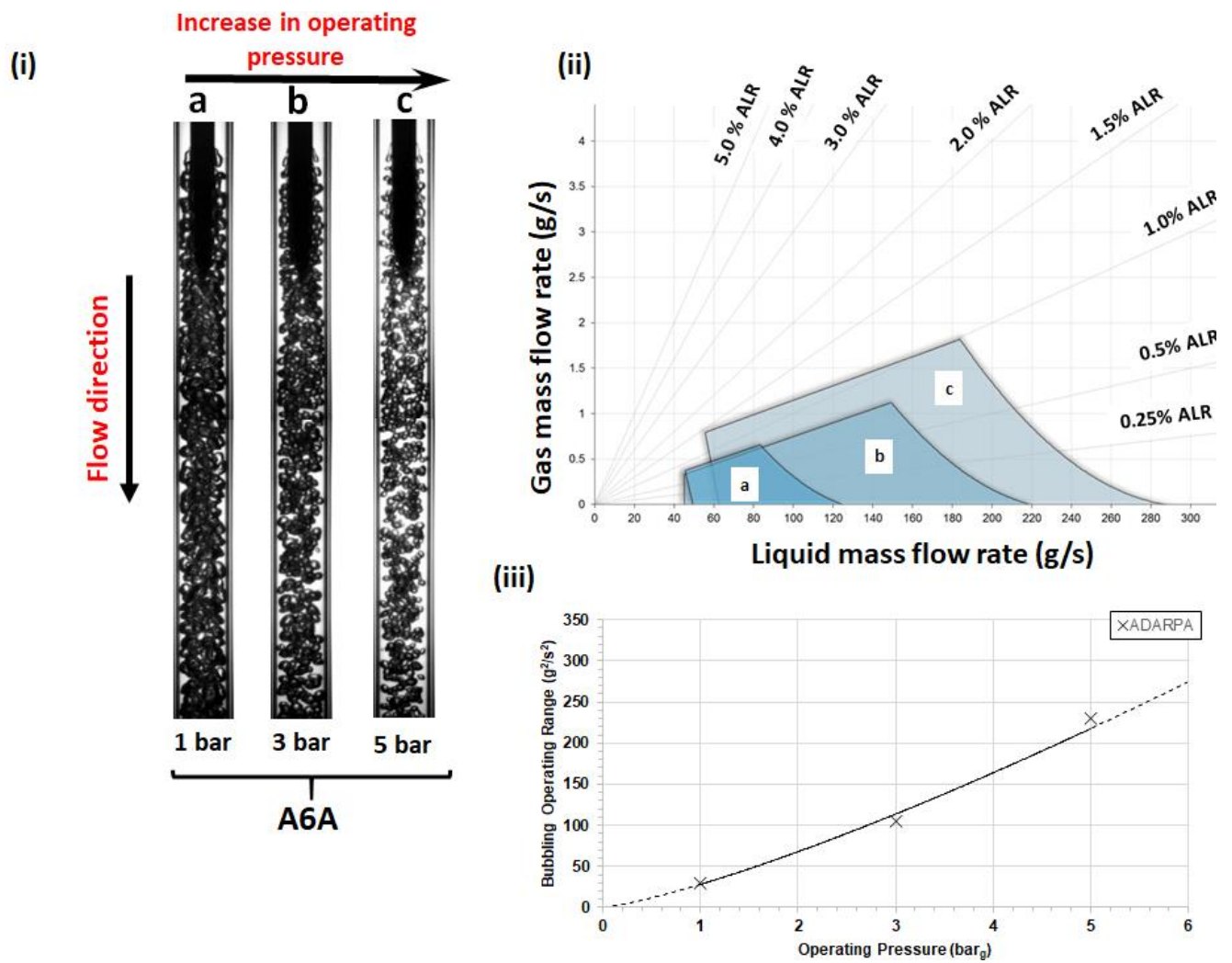


Figure 10. (i) Comparable observations of varying operating pressure for A6A: a) 1 bar, 253 g/s, 0.12% ALR; b) 3 bar, 251 g/s, 0.12% ALR; c) 5 bar, 251 g/s, 0.12% ALR. Liquid Baker parameter for all four cases is around:  $802.54 \text{ kg/m}^2\text{s}$ . (ii) Effect of operating pressure on bubbling operating range, with respect to the fluid mass flow rates: a) 1 bar (b) 3 bar; c) 5 bar. (iii) Dependence of mixing chamber diameter on bubbling operating range.

<b>Experimental Parameter</b>	<b>Aerator orifice diameter comparison</b>	<b>Aerator area comparison</b>	<b>Mixing chamber diameter comparison</b>	<b>Operating pressure comparison</b>
Discharge valve setting (g/s)	<b>30-290</b>	<b>30-290</b>	<b>30-290</b>	<b>30-225</b> <b>30-130</b>
ALR (%)	<b>0-5</b>	<b>0-5</b>	<b>0-5</b>	<b>0-5</b>
Aerator Geometry	<b>A1A, A2A, A3A, A6A</b>	<b>A4A, A5A, A6A, A7A</b>	<b>A6A</b>	<b>A6A</b>
Mixing chamber diameter (mm)	<b>20</b>	<b>20</b>	<b>14, 20, 25</b>	<b>20</b>
Operating pressure (bar)	<b>5</b>	<b>5</b>	<b>5</b>	<b>1,3,5</b>

Table 1. ADARPA atomizer configurations and flow setting employed to study the effect of various independent parameters on the internal flow